UNCLASSIFIED

AD _____

DEFENSE DOCUMENTATION CENTER

FOR

SCIENTIFIC AND TECHNICAL INFORMATION

CAMERON STATION ALEXANDRIA, VIRGINIA

UNCLASSIFIED

PROJECT SQUID

TECHNICAL REPORT NTI-1-C

SQUID CONFERENCE ON

ATOMIZATION, SPRAYS, AND DROPLETS

held at

NORTHWESTERN TECHNOLOGICAL INSTITUTE

SEPTEMBER 24-25, 1953

Project SQUID is a cooperative program of basic research in Jet Propulsion. It is supported jointly by the United States Army, Navy, and Air Force and is administered by the Office of Naval Research through contract N6-ori-105, Task Order 111 NR-098-038.

February 1955

Technical Report NTI-1-C

PROJECT SQUID

A COOPERATIVE PROGRAM
OF FUNDAMENTAL RESEARCH
AS RELATED TO JET PROPULSION
FOR THE
OFFICE OF NAVAL RESEARCH, DEPARTMENT OF THE NAVY
OFFICE OF SCIENTIFIC RESEARCH, DEPARTMENT OF THE AIR FORCE
AND THE
OFFICE OF ORDNANCE RESEARCH, DEPARTMENT OF THE ARMY

SQUID CONFERENCE ON

ATOMIZATION, SPRAYS, AND DROPLETS

held at

NORTHWESTERN TECHNOLOGICAL INSTITUTE

SEPTEMBER 24-25, 1953

JAMES FORRESTAL RESEARCH CENTER
PRINCETON UNIVERSITY
PRINCETON, NEW JERSEY

LIQUID CONFERENCE ON ATOMIZATION, SPRAYS, AND DROPLETS
Northwestern Technological Institute
September 24-25, 1953

CONTENTS

SQUID CONFERENCE ON ATOMIZATION, SPRAYS, AND DROPLETS
Northwestern Technological Institute
September 24-25, 1953

S&UID CONFERENCE ON ATOMIZATION, SPRAYS, AND DROPLETS
Northwestern Technological Institute
September 24-25, 1953

Foreword

In an attempt to stimulate communication among the many groups working on droplets, sprays and atomization, Project S&UID undertook to sponsor a conference devoted to this area of study. The conference took place at Northwestern University on September 24 and 25, 1953. Most of the work involved in preparation and staging was ably carried out by Professor George Lamb and his associates in the Chemical Engineering Department of the Northwestern Technological Institute. S&UID takes this opportunity of registering its appreciation for these efforts and for the cooperation and hospitality offered by the University.

As initially conceived, the conference was to be devoted largely to more or less informal review and discussion of various programs and topics relating the formation of sprays and droplets, their properties, and their applications. A primary objective was to have as complete representation as possible of all the groups active in spray and droplet research together with representatives of sponsoring agencies in order that future work in the field might be planned with some discretion, and minimum duplication.

Originally, publication of the proceedings of the meeting was not contemplated. It was believed that more complete participation might be achieved by encouraging informal discussion and by sparing contributors the chore of preparing formal manuscripts. Since the meeting there have been a large number of requests for some sort of summary. This report is in response to these requests. It includes abstracts of most of the talks and complete papers for four of them. In some cases it has not been possible to obtain even abstracts. The reader is referred to the authors in these instances. It is hoped that this summary of the conference proceedings, even though incomplete, will serve a useful purpose.

Report Number: SQUID Technical Report NTI-1-C

Title: SQUID Conference on Atomization, Sprays, and Droplets, Northwestern Technological Institute, September 24-25, 1953.

Author: None

Abstract

This report is a summary of the proceedings of a conference on Atomization, Sprays, and Droplets sponsored by SQUID at Northwestern Technological Institute in September 1953. Seventeen papers and discussions were presented. Abstracts or references to each are given. Four of the papers are given in entirety.

SQUID CONFERENCE ON ATOMIZATION, SPRAYS, AND DROPLETS
Northwestern Technological Institute
September 24-25, 1953

Paper Number 1

REVIEW OF EXPERIMENTS AND EMPIRICAL CORRELATIONS RELATING TO THE PRODUCTION OF SPRAYS

By W. R. Marshall, Jr.
University of Wisconsin

No abstract of the paper as presented is available. However, the material covered will appear as part of a Chemical Engineering Progress Monograph by Dr. Marshall on Atomization and Spray Drying. This monograph will be published by the American Institute of Chemical Engineers and is now in process.

S.UID CONFERENCE ON ATOMIZATION, SPRAYS, AND DROPLETS
Northwestern Technological Institute
September 24-25, 1953

Paper Number 2

REVIEW OF THEORETICAL AND MATHEMATICAL ANALYSES OF THE PERFORMANCE OF ATOMIZING NOZZLES

By R. Laster and M. Doumas
General Foods Corp.
Hoboken, N. J.

No abstract of this paper is available. The material is included in a paper by the authors appearing in Chemical Engineering Progress Volume 49, Number 10, pages 518-526, October 1953.

SQUID CONFERENCE ON ATOMIZATION, SPRAYS, AND DROPLETS
Northwestern Technological Institute
September 24-25, 1953

Paper Number 3

CHARACTERISTICS OF SPRAYS AND DROPLETS

By J. Mason Pilcher
Battelle Memorial Institute

The cascade-impactor method has been the subject of experimental study at Battelle during the past 2 1/2 years. A review of this work is presented. In this device, droplets in a moving air stream impact upon a slide placed in their path provided the inertia of the particles is sufficient to overcome the drag exerted by the air stream that must move around the slide. As the mist is drawn through the various stages of the impactor, the speed of the stream and therefore the efficiency of impaction increase and a size classification of droplets is accomplished. The Battelle instrument consists of six jet stages and a seventh filter stage arranged in tandem fashion. After this instrument is once calibrated, rapid determinations of drop size distribution may be made by using gravimetric, colorimetric, fluorometric or radiochemical methods of analysis, instead of the tedious procedure of microscopic counting. The impactor is most suitable in the size range of about 1 to 50 microns.

The movement of an individual droplet issuing from a spray nozzle is analyzed. In this review, it is shown how the motion depends upon the initial velocity of the drop and the drag due to the surrounding air. Drag coefficients of reasonable accuracy are available in the literature; however the analysis of the motion is greatly complicated by the period of acceleration and the distortion of the drop.

Additional experimental data, especially high-speed photography of droplets ejected at high velocities are required for a better knowledge of the dynamic behavior of droplets. The spinning-disk atomizer is suggested as an excellent tool for use in studying the trajectory and velocity of droplets. (Note: Complete paper in Appendix 1)

SECOND CONFERENCE ON ATOMIZATION, SPRAYS, AND DROPLETS
Northwestern Technological Institute
September 24-25, 1953

Paper Number 4

DROP SIZE DISTRIBUTIONS AND THEIR AVERAGES

By Ralph E. Thomas
Battelle Memorial Institute

In the current literature, there are several types of distributions which are of importance in describing the size consist of sprays. These distributions arise naturally in the course of experimental investigations employing different techniques. The specific distributions frequently employed in droplet statistics are: the normal distribution, the Log-normal distribution, the distributions of Rosin-Rammler and Nukiyama-Tanasawa. Having chosen a particular type of distribution function, the constant parameters may be computed so that the curve gives the best fit to the data. Analytical methods should supplement the graphical methods in the final determination of the values of the parameters. The customary use of relative error as a measure of the difference between theoretical and observed results is not adequate when probability considerations are involved. Unless the systematic errors can be determined and their effects eliminated, the fundamental problem of droplet statistics cannot be solved.

(Note: Complete Paper in Appendix 2)

SQUID CONFERENCE ON ATOMIZATION, SPRAYS, AND DROPLETS
Northwestern Technological Institute
September 24-25, 1953

Paper Number 5

REVIEW OF MASS AND ENERGY TRANSFER BETWEEN LIQUID DROPLETS AND SURROUNDING GASES

By Charles C. Graves and D. W. Bahr
National Advisory Committee for Aeronautics
Cleveland, Ohio

Close agreement between predicted and experimental evaporation rates of single drops in quiescent surroundings has been reported. The Langmuir equation has been verified for the evaporation of small drops in room air. The Fuchs equation for evaporation of small drops at low ambient pressures has been confirmed experimentally. The evaporation of single drops in high temperature surroundings is limited to the special case of single drops burning in quiescent atmospheres. Good agreement between theory and experiment was obtained.

Semi-empirical correlations for steady state forced convection evaporation from single drops of pure liquid are available in terms of either the heat or mass transfer equations. Drop surface temperatures may be determined for simultaneous solution of these equations or from a correlation in terms of the liquid boiling point for the higher temperature evaporation conditions. Theoretical heat or mass transfer coefficients for spheres are in approximate agreement with experiment.

Some data are available on the effect of both dissolved and suspended solids on the evaporation of water drops. No suitable data are available on the evaporation of wide boiling range hydrocarbons.

Calculations have indicated that the unsteady state evaporation may represent an appreciable portion of the total evaporation time. However, little experimental work has been done on this phase of the evaporation process.

Theoretical analyses of fuel spray evaporation have been made with

the assumption of zero relative drop-air velocities. Little experimental work on fuel spray evaporation has been done. To date no correlation between single drop and total spray evaporation has been obtained.

(Note: Complete Paper in Appendix 3)

SQUID CONFERENCE ON ATOMIZATION, SPRAYS, AND DROPLETS
Northwestern Technological Institute
September 24-25, 1953

Paper Number 6

FUEL SPRAY SPREADING AND EVAPORATION IN A FLOWING AIR STREAM

By Donald W. Bahr
National Advisory Committee for Aeronautics
Lewis Flight Propulsion Laboratory
Cleveland, Ohio

The evaporation rate and degree of fuel spreading of gasoline-type sprays were investigated over the range of inlet-air conditions common in ram-jet and tailpipe engines. This study was conducted by injecting isooctane contrastream from a simple-orifice nozzle into air flowing through an 8-inch diameter duct. Both the total and liquid fuel distributions across the duct were determined at various positions downstream of the fuel injector by sampling measurements. Some similar data were also obtained from tests in a 16-inch diameter ram-jet engine.

The influence of each of six experimental parameters was systematically determined, as follows: The measurements were taken at axial distances of 5, 10, and 18 inches from the nozzle over the ranges of inlet-air temperatures and velocities of 540-960° R and 100-350 feet per second, respectively. The ambient air pressure was varied from 18 to 35 inches of mercury absolute, nozzle diameters of 0.024, 0.033, and 0.041 inches and three fuel injection pressure differentials, 25, 55, and 85 psig were utilized.

Over these ranges of conditions, the evaporation rate and the degree of fuel spreading were correlated in terms of the six experimental parameters. The extremely large influence of air temperature on the spray vaporization was demonstrated by this analysis. The expression relating the fuel spreading to the experimental variables indicated that the spray residence time was the most important consideration in determining the degree of spreading.

The results of this investigation are limited to the case of upstream injection of isooctane from simple orifice nozzles. However, the relationships can probably be extended to any gasoline-type fuel without serious error. The fuel spreading results are also limited since these data were obtained with turbulence less than that to be expected in engines. Therefore, for application to engine design, these results represent the minimum degree of fuel spreading. The major contribution of this study was to provide an indication of the relative importance of each of the inlet-air and fuel-injection parameters on the evaporation and mixing of fuel injected into high velocity airstreams.

LIQUID CONFERENCE ON ATOMIZATION, SPRAYS, AND DROPLETS
Northwestern Technological Institute
September 24-25, 1953

Paper Number 7

REVIEW INSTRUMENTATION AND METHODS OF EXPERIMENTAL STUDY

By J. L. York
University of Michigan

No abstract of this paper is available. Of particular interest was the discussion of the electronic counting probe technique for studying sprays which has been developed by Dr. York. The reader is referred to the author for further information.

SQUID CONFERENCE ON ATOMIZATION, SPRAYS, AND DROPLETS
Northwestern Technological Institute
September 24-25, 1953

Paper Number 8

AN APPARATUS FOR SUSPENDING SMALL DROPLETS OF LIQUID IN SPACE

By J. A. Bolt
University of Michigan

This paper describes a piece of apparatus that is being used to suspend single droplets of liquid in space. The method, unlike all previous methods, does not depend on physical contact between the drops and a solid filament but obtains the necessary forces for holding the drop from a rising column of air and a standing ultrasonic field. The air column supplies the necessary drag force to overcome the force of gravity while the ultrasonic field provides both lateral and vertical forces to hold the drop in a fixed position.

To generate the air column, a vertical wind tunnel was designed which consists of a divergent section to decrease the velocity of the supply air, a calming section to reduce turbulence, and a convergent nozzle to supply a low turbulence column of air to the ceramic transducer described below. Auxiliary apparatus associated with the wind tunnel are a pressure reducing valve, surge tank, air filter, air heater, and flow orifice.

The ultrasonic field is generated by a cylindrical tube barium titanate ceramic transducer. The tube is four inches long and has an inside diameter of one and five-eights inches. Two windows are cut in the wall so that the drop can be illuminated and photographed. Power for the transducer is supplied by a forty-five watt amplifier which is fed by an audio oscillator with a range to 40,000 cps.

In operation the ceramic transducer is placed above the outlet of the wind tunnel nozzle, and a low velocity air stream is started through the transducer. The oscillator is then varied until the desired resonant frequency of the tube is reached, at about 37,000 cps. This is detected by a needle which is suspended in the tube. Before

resonance is reached, the needle shows no preferential position as it is moved within the tube, but at resonance, the needle is held quite firmly along one of the nodes in the ultrasonic field. A slight deflection of the string used to suspend the needle will not move the needle.

When the tube is at proper resonance, droplets of liquid are shaken into the ceramic tube from an eye dropper, and the air velocity is adjusted until a droplet is suspended in the correct node used for observation. As the drop evaporates, the air velocity is manually decreased to keep the drop in position opposite the observation window.

Photographic records of evaporating drops are made with an Army Air Forces 16mm gun camera which is capable of speeds of 16, 32, and 64 frames per second. To obtain the necessary magnification, an extension tube for the lens has been built, giving a magnification of about 4X. The extension tube also contains a half silvered mirror and ground glass so that the drop can be observed as it is being photographed.

LIQUID CONFERENCE ON ATOMIZATION, SPRAYS, AND DROPLETS
Northwestern Technological Institute
September 24-25, 1953

Paper Number 9

MEASUREMENT OF WET BULB TEMPERATURE IN MISTS

By E. W. Comings
Purdue University

An analysis of the evaporation of a water spray in a simplified flow system, which has in fact a prototype of a new design of spray dryer, is presented. In addition, a new instrument, the pneumatic thermometer and hygrometer which is useful in studies of sprays, is described. The meaning of the pressure measured by a Pitot tube in a flowing spray-gas mixture is analyzed mathematically.

The water spray was evaporated in a prototype of the high velocity spray dryer. This dryer consisted of a two-fluid atomizer, with hot air atomizing the liquid feed, which discharged into a second concurrent stream of hot air. It represented an attempt to utilize the rapid heat and mass transfer during atomization in spray drying. The momentum, mass and heat transfer in this system were followed in detail by measuring the velocity, gas temperature, water temperature, liquid water concentration, and humidity at a large number of points in each of six successive cross-sections. The results of these measurement for a single case of water evaporating into air are presented and analyzed. Water was atomized to droplets of 20 microns mean diameter by a stream of air at 400°F. moving at 850 ft./sec. This stream was subsequently mixed with a stream at 280°F. moving at 30 ft./sec. The atomizing nozzle was 0.500 inches in diameter and the coaxial drying chamber was 6 inches in diameter. Evaporation of the spray was complete within 30 inches downstream from the nozzle. The data were analyzed in terms of Reichardt's theory of free turbulence. The spreading coefficients obtained were in the same range as those obtained by other investigators, although not in close agreement. The spreading coefficient for water droplets was measured

and found to be considerably less than that for gas under the same conditions.

The pneumatic thermometer and hygrometer was developed to permit the measurement of the gas temperature and humidity in a gas-spray mixture. This instrument relies on the changes in pressure and temperature as a sample of the mixture is passed through as orifice, then a heater, a second orifice, a drying bed, and finally a third orifice. Details of the development and testing of this new instrument are presented.

A mathematical analysis of the performance of a Pitot tube in a flowing spray-gas mixture is presented. This analysis gives a method of determining the magnitude of the error caused by the droplets entering the Pitot tube. It is shown that this error is dependent upon drop size and Pitot-tube diameter, and that a series of Pitot tubes may therefore be used to determine drop size distribution in a gas-borne spray. Such a device awaits practical development.

Microfilm copies of the thesis are available through University Microfilm, Inc., Ann Arbor, Michigan.

Note: The material covered by Dr. Comings was taken from a thesis entitled "Sprays in Hot Turbulent Streams" by Clarke Lincoln Coldren, Department of Chemistry and Chemical Engineering, University of Illinois. The thesis has been deposited with the University of Illinois Library. Microfilm copies are available through University Microfilm Inc., Ann Arbor, Michigan.

SQUID CONFERENCE ON ATOMIZATION, SPRAYS, AND DROPLETS
Northwestern Technological Institute
September 24-25, 1953

Paper Number 10

GAS ABSORPTION AND AEROSOL COLLECTION IN A VENTURI ATOMIZER

By H. F. Johnstone, R. B. Feild[1], and M. C. Tassler[2]
University of Illinois
Urbana, Illinois

The success of the Venturi scrubber as an efficient device for contacting large volumes of gases for absorption and dust collection has made important this study of the rates and mechanism of transfer in the spray zone. The scrubber consists of a conventional Venturi section into which the scrubbing liquid is injected at the throat, followed by a cyclone for removing the liquid droplets containing the material collected. The high velocity of the gas stream relative to the liquid causes atomization into a spray of many small droplets which present a large surface for mass transfer.

Gas film coefficients were measured for the absorption of sulfur dioxide by an alkaline solution by collecting the spray droplets by an impact nozzle surrounded when necessary by a stream of inert gas. Exposure times for the liquid were in the range from 0.1 millisecond to 1 second. Similar methods were used for measuring the liquid film coefficients for the desorption of carbon dioxide from water, and the rate of collection of aerosol particles by water spray. The aerosols were produced by the condensation of dibutylphthalate vapor, or by the chemical reaction of ammonia gas with dilute SO_2 or HCl in air. The particle size of the aerosols were nearly uniform and varied between 0.27 and 1.22 micron mean diameter for the three materials used.

---

[1]Present address: Eastern Laboratory, du Pont Company, Gibbstown, New Jersey.
[2]Present address: Film Division, du Pont Company, Buffalo, New York.

The Venturi sections used were made of Lucite with throats 1-1/8 to 1-1/2 inches in diameter and 1-1/2 to 5 inches long and with 4° to 7° divergence angles.

The observed individual absorption film coefficients, $k_L a$ and $k_G a$, are very high near the liquid source. The value of the former for CO_2 falls off abruptly from a maximum about one inch downstream which is in the range of 5000 to 17,000 lb. moles/(hr.)(cu.ft.)(lb. mole/cu.ft.) to almost zero at four inches. The average gas film coefficient for SO_2 is in the range of 300 to 1400 lb. moles/(hr.)(cu.ft.)(atm.) at 3.5 inches from the liquid source and decreases more slowly with distance as the interfacial velocity decreases. Both coefficients are functions of gas velocity and liquid-gas ratio. Estimates of the surface area of the liquid droplets based on atomization equations permit calculating the film coefficients k_L and k_G, and indicate the extremely rapid transfer rates in the atomization zone. Possible applications of Venturi atomizers are suggested for difficult absorption problems.

Aerosol collection by spray droplets in the atomization zone takes place primarily by the inertial impaction mechanism. The efficiency of collection depends on the inertia of the aerosol particles and is practically independent of small natural electrostatic charges on the droplets and the particles, and of their diffusivity and wettability. The rate of collection falls off rapidly with distance from the spray nozzle as the relative velocity of the gas and liquid decreases. A theoretical equation based on inertial forces gives excellent correlation of the collection efficiencies for all of the aerosols studied.

SQUID CONFERENCE ON ATOMIZATION, SPRAYS, AND DROPLETS
Northwestern Technological Institute
September 24-25, 1953

Paper Number 11

FUEL INJECTION PROBLEMS IN TURBOJETS

By H. A. Fremont
General Electric Company
Aircraft Gas Turbine Division
Cincinnati 15, Ohio

No abstract of this paper is available. Mr. Fremont gave a talk, illustrated by slides, discussing in general the technology of turbojet fuel combustor applications, a few of the present problems, and some areas in which future research is needed.

SQUID CONFERENCE ON ATOMIZATION, SPRAYS, AND DROPLETS
Northwestern Technological Institute
September 24-25, 1953

Paper Number 12

INJECTION IN AFTERBURNING TURBOJETS

By D. G. Samaras
Wright Patterson Air Force Base
Dayton, Ohio

1. The injection of fuel in afterburning turbojets has a profound effect upon the performance and the operational stability of the afterburner.

2. Generally speaking, at least two operational cases of afterburners are apparent:

   a. The afterburner operates only a short time of the total flight time.

   b. The afterburner operates during most of the whole flight time.

3. The design requirements of the above distinct cases are entirely different.

4. The types and geometric location of the injectors in the afterburner have a great influence upon:

   a. Combustion efficiency

   b. Pressure losses

   c. Temperature distribution

   d. Instability

5. The two main modes of upstream and downstream injection may result in the following five types of afterburning:

   a. Preturbine injection

   b. Afterburning upstream injection with flameholders

   c. Afterburning upstream injection without flameholders (turbine stabilization)

d. Afterburning downstream injection with flame holders

e. Afterburning downstream injection with tail-cone-end injector

6. The advantages and disadvantages of the above types are discussed. A hypothesis of the screech instability is given, and the influence of the injection process upon this instability is discussed. The influence of injection during acceleration and deceleration is also dealt with.

Note: Complete Paper in Appendix 4

SQUID CONFERENCE ON ATOMIZATION, SPRAYS, AND DROPLETS
Northwestern Technological Institute
September 24-25, 1953

Paper Number 13

FUEL INJECTION PROBLEMS IN RAMJETS

By J. P. Longwell
Standard Oil Development B

Ramjet fuel is typically injected into the high velocity air at the diffuser exit through an atomizing-nozzle of moderate pressure drop. The air stream velocity is generally several hundred ft./sec. so that the relative velocity between fuel and air and therefore the atomization is largely controlled by the air velocity. Air atomization data using pressure atomizing nozzles for a variety of air densities are therefore of particular interest. The drops formed are in the 5-40 micron range. Such drops are capable of following some of the turbulent velocity fluctuations and accelerate very quickly to stream velocity. The rate of evaporation and turbulent diffusion of such small drops requires further study and may not be easily predicted from data obtained on large drops.

SQUID CONFERENCE ON ATOMIZATION, SPRAYS, AND DROPLETS
Northwestern Technological Institute
September 24-25, 1953

Paper Number 14

APPLICATION OF SPRAY TECHNOLOGY TO LIQUID PROPELLANT ROCKETS

By C. C. Miesse
Aerojet-General Corporation
Azusa, California

Combustion in the thrust chamber of a liquid propellant rocket is a very complex phenomenon, so that it is almost impossible to determine which of the many processes which occur is the determining factor for performance, heat transfer, or stability. However, on the basis of the time elapsed during each of the processes, it is logical to assume that the less rapid physical processes of jet disintegration, evaporation and diffusion should have a greater effect than the rapid chemical conversion of the unburned propellants into the products of combustion. It is interesting to note that the theories of combustion stability - as presented by Gunder and Friant, Summerfield, and Crocco, for instance - are all based on the concept of the time lag which exists between the injection of the propellants and their subsequent conversion, thus giving substantial confirmation to the above assumption regarding the relative importance of the physical processes.

Recognizing the importance of the physical processes, the Aerojet-General Corporation has undertaken several experimental and theoretical investigations of jet disintegration, droplet evaporation, and gaseous diffusion.

An experimental and theoretical study of jet disintegration in ambient air resulted in some interesting correlations, on the basis of previously published theories, of data obtained from two types of injectors (similar to conventional rocket injectors), and using two different liquids - water and liquid nitrogen. The latter liquid was chosen in order to study what effects, if any, were caused by a high evaporation rate, and it was found

that the apparent differences between the water and liquid nitrogen data could be ascribed solely to the difference between primary and disintegration and secondary atomization. The data included wave-length of disturbance, maximum drop-size, and break-up length of the jet. Additional experiments are currently under way to determine the mutual effects of several colinear jets, and the effect of variations in ambient pressure.

A second phase of the study has been a theoretical investigation of the ballistics of burning droplets. By assuming that the drag coefficient varies inversely as the Reynolds number, that the velocity of the surrounding gases varies directly with distance downstream of the injector, and the surface area of the burning droplet varies linearly with time, Newton's law of motion was used to determine the velocity profile, lifetime, and proper initial size of the droplets for various initial velocities and ratios of kinematic viscosity to evaporation rate. Application of the same general method to the similar problems of evaporation or burning in a gas stream whose velocity varies linearly with distance is outlined.

Two aspects of the effect of diffusion on the stability of a rocket system are indicated, and it is concluded that the needs and opportunities for further research are essentially unlimited.

SQUID CONFERENCE ON ATOMIZATION, SPRAYS, AND DROPLETS
Northwestern Technological Institute
September 24-25, 1953

Paper Number 15

VAPORIZATION OF FUEL DROPLETS IN A DIESEL ENGINE

By P. S. Myers, O. A. Uyehara and M. M. El Wakil
University of Wisconsin
Madison, Wisconsin

Theoretical relationships were developed from basic heat-transfer and diffusion theories by which the history of a fuel droplet injected in heated air can be predicted. The droplets are assumed to be injected with a certain initial velocity relative to the air and are slowed down by aerodynamic drag forces, the drag coefficients being taken as those for solid spheres. The vaporization time is roughly divided into two portions, the unsteady state, or the time spent by the droplets in heating-up to their wet-bulb temperatures, corresponding to the air ambient conditions, and the steady state where the droplets remain at the wet-bulb temperatures until complete vaporization takes place. The unsteady state portion has been found to be of importance in most cases.

The equations assume (a) no interaction between droplets (b) the air ambient conditions remain unchanged throughout the vaporization process and (c) spherical symmetry of the droplets and the air-vapor film surrounding them exists at all times. The equations are integrated by a stepwise procedure in which their lifetime is divided into small increments during which the droplet radius, temperature and velocity relative to the air are assumed constant. It was found that the equations yield reasonably accurate results when compared with experimental values obtained for fairly large drops vaporizing in heated atmospheric air.

While the droplets are vaporizing in the unsteady state, they reach such a temperature where their vapor pressure is high enough so that a stoichiometric mixture of air and vapor is first formed in the film at the droplet surface and having a temperature equal to that of the liquid.

As the droplet is heated more, its vapor pressure increases and the stoichiometric mixture moves away from the droplet into a higher temperature region. The temperature of the stoichiometric mixture reaches a steady state at essentially the same time the droplet reaches its wet-bulb temperature. Thus, the stoichiometric mixture must reach its ignition temperature while the droplet is in the unsteady state if the droplet is to ignite at all. The time spent by the droplet until the stoichiometric mixture reaches its ignition temperature is defined as the vaporization portion of the total physical ignition delay period.

This portion, d, of the physical ignition delay, calculated by the above method was found to approximately follow an equation of the form

$$d = c_1 e^{\frac{c_2}{T}}$$

where T is the absolute air temperature and c_2 is the slope of this line when plotted on semi-log graph paper. c_2 was found to be in the range of the slopes of the physical ignition delays obtained graphically from experimental combustion bomb data. It is hoped that continuation of this theoretical study together with experimental bomb data on pure hydrocarbon fuels will help in formulating a rational theory for physical ignition delays.

In developing the above equations the thermal conductivity of the liquid droplets was assumed to be infinite. This was verified experimentally by the absence of a temperature gradient inside the drops. Explanation was found in the internal circulation within the drops which were observed during the experiments. This circulation induced enough fluid mixing to effectively make the thermal conductivity infinite. Circulation was found to be in a doughnut shaped pattern with the fluid near the surface of the drop moving in the same direction as that of the air stream and in the opposite direction at the center. A film showing the circulation was prepared under an NACA contract and is on file at the NACA Washington Headquarters.

LITERATURE

1. El Wakil, M. M., Uyehara, O. A., and Myers, P. S.: A Theoretical Investigation of the Heating up Period of Injected Fuel Droplets Vaporizing in Air. NACA TN 3179

2. El Wakil, M. M., Priem, R. J., Brikowski, H. J., Myers, P. S and Uyehara, O. A.: Experimental and Calculated Temperature and Mass Histories of Vaporizing Fuel Drops. A report prepared under NACA contract NAw-6278, The University of Wisconsin, April 1954

3. Wentzel, W.: Zum Zundvorgang im Dieselmotor. Forschung auf dem Gebiete des Ingenieurwesens, May-June 1935, pp. 105-115

4. Gerrish, H. C., and Ayer, B. E.: Influence of Fuel Oil Temperature on the Combustion in a Prechamber Compression Ignition Engine. NACA TN 565, April 1936

5. Jost, W.: Explosion and Combustion Processes in Gases. McGraw Hill Book Co., First edition, 1946

SQUID CONFERENCE ON ATOMIZATION, SPRAYS, AND DROPLETS
Northwestern Technological Institute
September 24-25, 1953

Paper Number 16

FUEL INJECTION PROBLEMS IN OTTO CYCLE ENGINES

By W. L. Meyers
Pennsylvania State College
State College, Pennsylvania

No abstract of this paper is available. Professor Meyers has kindly agreed to make available to all those attending the conference who request it a copy of the Bibliography of Sprays which was sponsored by the Texas Company.

SQUID CONFERENCE ON ATOMIZATION, SPRAYS, AND DROPLETS
Northwestern Technological Institute
September 24-25, 1953

Paper Number 17

CHEMICAL ENGINEERING APPLICATIONS

By H. F. Johnstone, W. R. Marshall,
J. L. York, E. W. Comings and G. G. Lamb

This item on the program was not a formal paper but comprised a round table discussion centering largely around the question of internal circulation within droplets. In addition, Professor Lamb reported on his work at Northwestern dealing with the evaporation of two component fluids atomized in pressure swirl nozzles and injected into stagnant heated air.

LIQUID CONFERENCE ON ATOMIZATION, SPRAYS, AND DROPLETS
Northwestern Technological Institute
September 24-25, 1953

Appendix Number 1

(Paper Number 3 In Toto)

CHARACTERISTICS OF SPRAYS AND DROPLETS

by

J. Mason Pilcher

Battelle Memorial Institute

September 1953

CHARACTERISTICS OF SPRAYS AND DROPLETS

by

J. Mason Pilcher

The primary purpose of atomizing a liquid is to increase its surface area. This is especially true when the liquid to be atomized is a fuel that must be vaporized for intimate mixing with air before combustion can take place. The most important physical characteristic of a spray, therefore, is drop-size distribution, because this characteristic determines surface area, rate of evaporation, and rate of combustion.

The extent to which atomization increases surface area is well illustrated by J. R. Joyce[1] by means of a simple example. A cubic centimeter of liquid, in the shape of a sphere, would have a diameter of 1.24 cm, and its surface area would be 4.83 sq cm. If this sphere is then atomized into one million equal-sized small spheres, each having a volume of 10^{-6} cc, each droplet would have a diameter of 0.0124 cm, and the total surface area of the one million droplets would be 483 sq cm, or one hundred times that of the original single sphere. The surface area per unit volume is, therefore, inversely proportional to the diameter of the droplets, for by reducing the drop size by a factor of 100, the total surface area is increased by a corresponding factor of 100.

Figure 1 shows these relations schematically. The usual methods of atomization result in the liquid being broken up even more finely than is indicated by this example, and, of course, a wide range of drop sizes results. A typical fuel spray would consist of droplets ranging in sizes from 1 micron (0.0001 cm) to 500 microns (0.05 cm), and each cubic centimeter

BASIS: ONE CUBIC CENTIMETER OF LIQUID

BEFORE ATOMIZATION	AFTER ATOMIZATION
	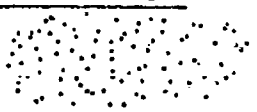
NUMBER OF DROPS = 1 DIAMETER = 1.24 CM AREA = 4.83 SQ CM VOL. PER DROP = 1 CU CM	NUMBER = 1,000,000 DIAMETER = 0.0124 CM AREA = 483 SQ CM VOL. PER DROP = 1×10^{-6} CU CM

FIGURE 1. EFFECT OF ATOMIZATION ON SIZE AND SURFACE AREA OF DROPLETS

of fuel would be divided into not just one million but tens of millions of droplets having a surface area of over a thousand sq cm per cc.

The instruments and experimental methods for measuring this important characteristic of drop size will be covered in a review paper tomorrow morning by Professor J. L. York; however, I shall include a brief discussion of only one method, the cascade-impactor method, which has been the subject of experimental study at Battelle during the past 2-1/2 years. Immediately following this paper Ralph E. Thomas will discuss the rather complex and controversial subject of mathematical representations of drop-size distributions.

The other major characteristic of sprays, in addition to drop size, is the dynamic behavior of the droplets after they leave the atomizing device. The characteristic of dynamic behavior involves such factors as the initial and terminal velocity of individual particles, the time and distance of travel before terminal velocity is attained, and the effects of particles upon each other in a concentrated spray.

First the experimental work with the cascade impactor will be discussed briefly, after which the dynamic behavior of droplets will be reviewed.

MEASUREMENT OF DROP-SIZE DISTRIBUTION WITH THE CASCADE IMPACTOR

As a part of the program of research on the burning characteristics of fuel mists, extensive work has been done on the development of the cascade impactor as an instrument for determining the drop-size distribution of atomized liquid fuel. The cascade-impactor method was chosen from among the various methods that you will hear described tomorrow morning because, after the instrument is once calibrated, rapid determinations of drop-size

distribution may be made by using gravimetric, colorimetric, fluorometric, or radiochemical methods of analysis, instead of following the tedious and time consuming procedure of microscopic counting.

Principle Of The Cascade Impactor

The cascade impactor operates on the principle that droplets in a moving air stream will impact upon a slide placed in their path provided the inertia of the particles is sufficient to overcome the drag exerted by the air stream that must move around the slide.

Figure 2 shows, schematically, what happens when a fine spray approaches a glass slide in one of the early stages of a cascade impactor. The large droplets impact on the slide, whereas the small droplets follow the air stream into the next jet which is smaller in diameter than the previous one and which thereby imparts a higher velocity to the stream of mist. At the higher velocity, smaller sizes of droplets will impact on the slide. The cascade impactor, therefore, accomplishes a size classification of droplets by increasing the speed and therefore the efficiency of impaction as the mist is drawn through the various stages of the impactor. K. R. May[2], in his pioneer work on the cascade impactor, used an instrument consisting of four stages placed at right angles to each other.

The Battelle No. 4 Cascade Impactor

The instrument now being used at Battelle, by James L. Harp, consists of six jet stages and a seventh filter stage, arranged in tandem fashion. A tandem arrangement was first used by T. Hale of the NACA.

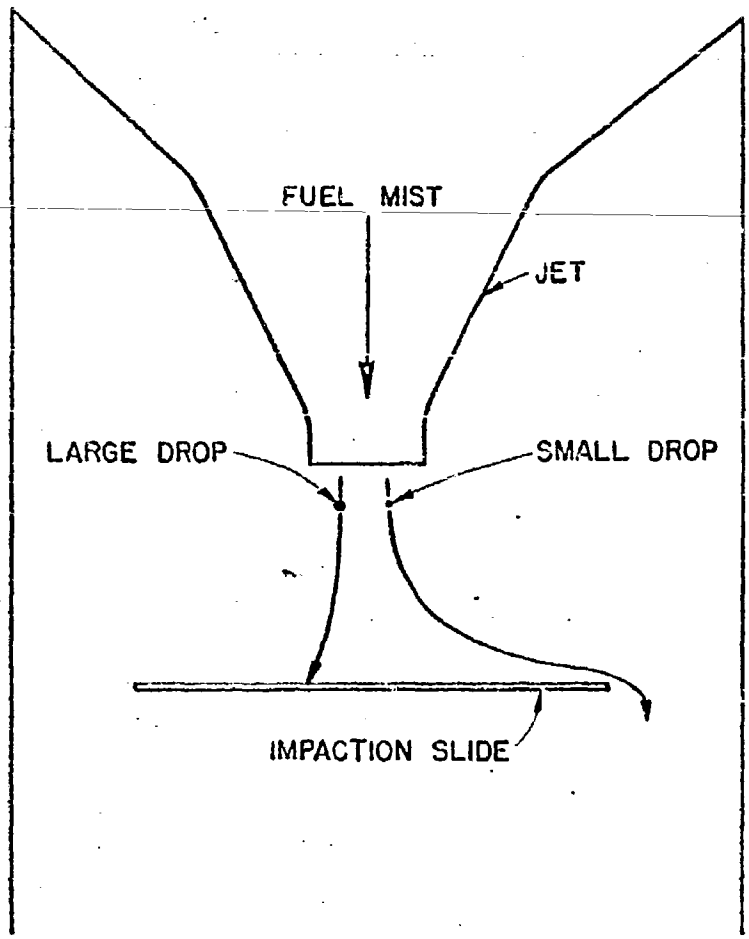

FIGURE 2. SCHEMATIC DIAGRAM SHOWING PRINCIPLE OF THE CASCADE IMPACTOR

Figure 3 shows an assembly drawing of this instrument which is designed to cover the size range of 3 to 40 microns by impacting the droplets on the six jet stages. A seventh filter stage removes most of the minus 3-micron material. A vacuum applied at the exit of the impactor draws the sample through the instrument at a fixed rate determined by a critical orifice meter.

Sampling of the spray is a difficult problem when using the cascade impactor and, for that matter, when using any apparatus for determining particle-size distribution. To insure that the sample will be as highly representative as possible, an "isokinetic" sampling procedure is followed. Isokinetic sampling is achieved when the velocity of the mist entering the sampling port of the impactor is maintained essentially equal to the velocity of the stream being sampled. The path of the mist remains practically unchanged as it enters the impactor, and discrimination against either the larger or smaller droplets is reduced to a minimum. A stationary mist obviously cannot be sampled isokinetically.

Calibration Of The Cascade Impactor

The objective in calibrating the cascade impactor is to establish the upper and lower size limits or size range of the droplets that collect on each stage. This is accomplished by sampling a mist over a short enough period of time to prevent coalescence of droplets, and measuring the diameter of all droplet on a slide or portion of a slide. Photomicrographs of the impaction slides may be projected by means of an enlarger-viewer to simplify greatly and improve the accuracy of calibration, which involves the measurement of about a thousand droplets per stage. A histogram for each slide is

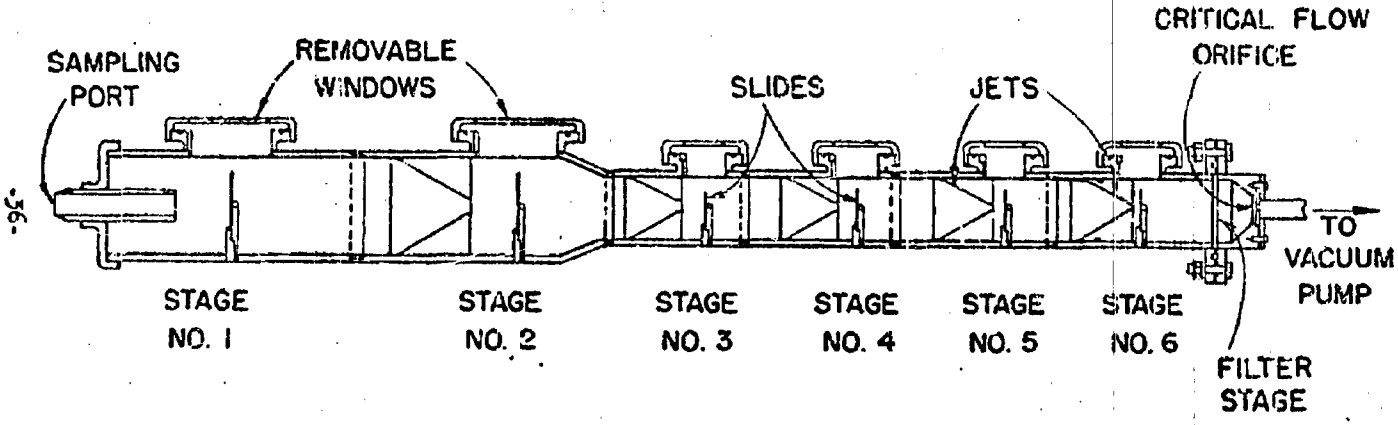

A 4294-A

FIGURE 3. BATTELLE NO. 4 CASCADE IMPACTOR

then prepared to establish the "cut-off" point which is the lower size limit for one stage and the upper size limit for the succeeding stage.

One of the major problems in the calibration of the impactor is that the cut-off point is not perfectly sharp, and a certain amount of overlap of drop sizes occurs between adjacent stages. This problem is resolved by defining the cut-off point as the size of drop such that an equal number of them will deposit on two successive stages.

Other factors involved in calibrating the cascade impactor are: (1) the use of a nonvolatile liquid, such as dibutyl phthalate, and (2) correction for the flattening of spherical droplets after impaction on the glass slide. Allowance for the flattening of the droplets is made by determining the "flattening coefficient", which is the factor by which the flattened diameter must be multiplied to obtain the diameter of the spherical drop before impact. The value of the flattening coefficient for droplets of dibutyl phthalate on clean glass slides, treated with a wetting agent, is 0.50 ± 0.01 based on determinations by three independent methods.

Once the cascade impactor is calibrated, and the upper and lower size limits for each slide are established, rapid determinations of drop-size distribution may be made by employing relatively rapid analytical methods to determine the weight of material impacted on each stage. Use of a tracer method employing a nonvolatile dye or fluorescent salt is recommended when the atomized liquid is appreciably volatile as is the case for all liquid fuels.

A Limitation Of The Cascade Impactor

A limitation of the cascade impactor that must not be overlooked is that it does not function satisfactorily when sampling coarse sprays.

The impactor is most suitable in the size range of about 1 to 50 microns. The high inertia of large particles of 100 microns' diameter may cause them to deviate markedly from the air flow lines before the first slide is reached and to deposit on the inside of the sampling tube or on the inner walls of the impactor, rather than on the glass slides. This wall loss generally amounts to less than 3 per cent for the small droplets, but wall loss may be as much as 10 or even 50 per cent for drops of 50 microns' diameter. The extent of wall loss should be determined experimentally for the specific test conditions imposed.

Conclusion Regarding The Cascade Impactor

When dealing with liquid dispersions in which all droplets are under 50 microns in diameter and when isokinetic sampling can be employed, the cascade impactor is an excellent instrument for determining drop-size distribution. The suitability of the instrument decreases as maximum drop size increases, owing to the deposition of large droplets on the inside of the sampling tube.

DYNAMICS OF DROPLETS

The time-distance-velocity relations of a drop depend upon two factors, (1) the initial velocity of the drop, and (2) the drag of the surrounding air into which the drop is injected. For large drops the initial velocity dominates the dynamics of the travel for an appreciable length of time, but small droplets attain the air velocity in an extremely short interval of time.

When a droplet moves relative to the surrounding air, a resistance or drag causes the droplet to accelerate or decelerate until its velocity approaches that of the air. When the particle is at rest, with respect to the air, the drag force is zero; but resistance is always present whenever the particle is in motion with respect to the air. This may be expressed by the basic equation

$$R = f(v,\dot{v})$$

where R is the resistance, v is the difference in velocity between the particle and the medium, and $\dot{v}$ is the acceleration of the drop.

The exact evaluation of this function is complicated in the case of the motion of droplets ejected at high velocity from an atomizing nozzle. The functional form for drag is complex and changes markedly over most of the range of interest for typical sprays; however, in the limited range where the droplets have slowed down and are moving with laminar motion, the simple Stokes' law applies. Consequently, only brief reference will be made to Stokes' law, with special emphasis on its limitations, after which the more complicated functions for drag will be reviewed.

Stokes' Law

The basic Stokes' law equation is:

$$R = 6\pi\mu r v$$

where μ is the viscosity of the fluid, r is the radius of the spherical particle, and v is the velocity of the particle relative to the medium, all in cgs units.

One of the principal applications of Stokes' law is the evaluation of the terminal velocity of freely falling particles. A constant terminal

velocity is achieved when the fluid resistance becomes equal in magnitude and opposite in direction to the resultant of all the other forces acting on the particle. Under the force of gravity, the equation for terminal velocity is[3,4],

$$v_m = \frac{2}{9} \frac{(\rho - \rho') r^2 g}{\mu}$$

where ρ and ρ' are the densities of the droplet and the medium, respectively, and g is the acceleration of gravity.

Stokes' law applies accurately only for particles moving with laminar motion which requires that the Reynolds number for the particle lie between 10^{-4} and 1. As a consequence, the practical range of application for droplets of unit density is about 1 to 80 microns[5]. Above this size special empirical equations have been developed to determine the terminal velocity of droplets up to 1000 microns[6].

Figure 4 shows the terminal velocity of water droplets for diameters of 3 to 1000 microns, which is the size range of greatest interest in the study of the dynamic behavior of sprays.

Table 1 shows values of the terminal velocity and of the "half-time", (t_h), for five sizes of droplets. "Half-time" is the time required for a particle, starting from rest, to attain one-half of the terminal velocity.

For practical purposes small droplets, under 20 microns' diameter, attain terminal velocity as soon as they begin to fall freely in air, and the distance traveled before attaining terminal velocity is insignificant. Consequently, the dynamic behavior of such droplets is wholly dependent upon the movement of the air stream in which they fall. Large drops fall several feet before the constant terminal velocity is closely approached.

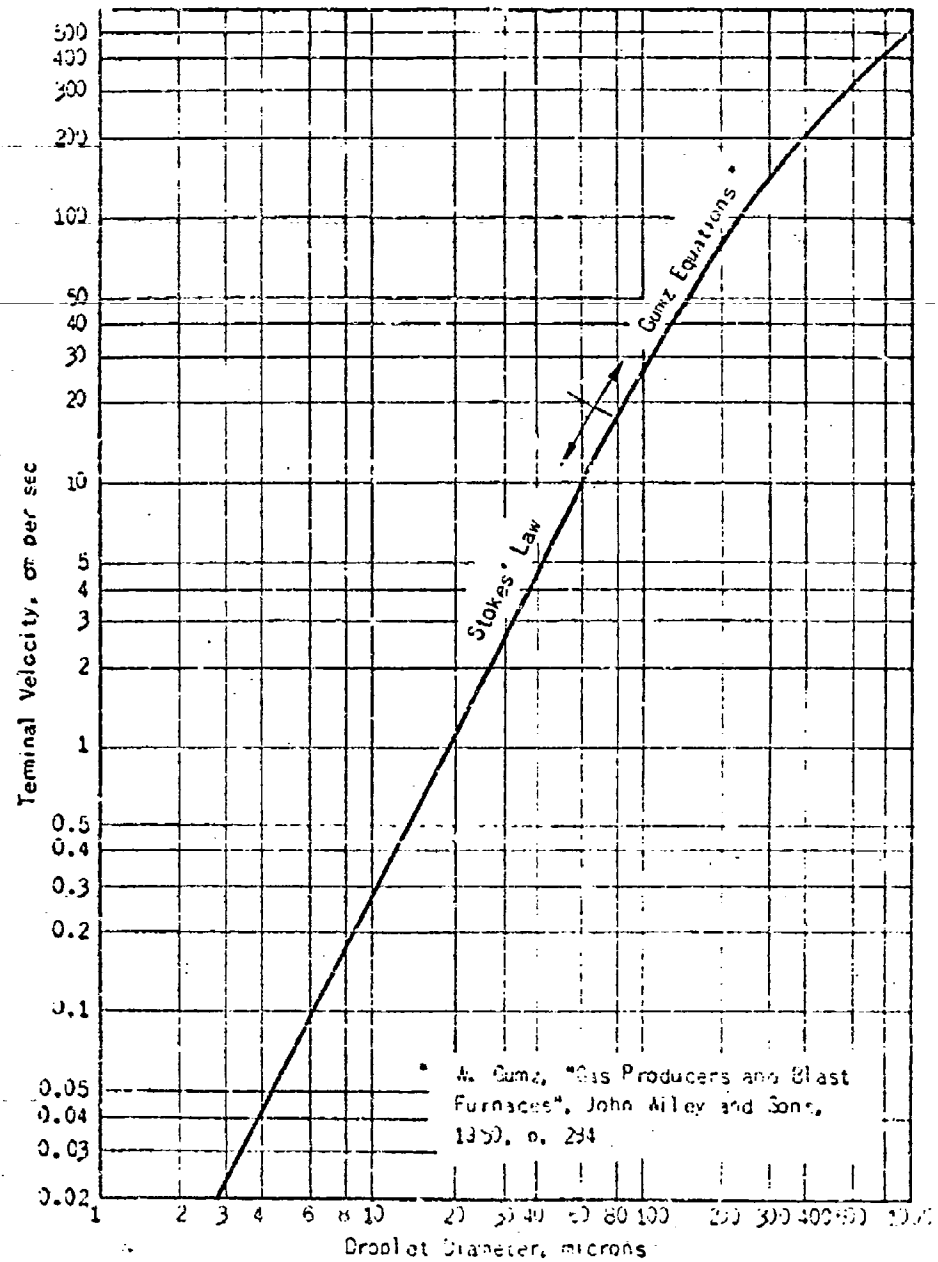

FIGURE 4. TERMINAL VELOCITY OF WATER DROPLETS IN AIR AT 70 F

3 3814-A

As mentioned previously, the droplets of a typical spray are seldom moving with laminar motion, as required by Stokes' law, except near the end of their trajectories. Consequently, the more complex and practical case of droplets moving at Reynolds numbers greater than 1 will be considered, principally from the standpoint of drag coefficient.

TABLE 1. TERMINAL VELOCITIES AND HALF-TIME FOR WATER DROPLETS IN AIR

Droplet diam, μ	Terminal velocity (v_m), cm/sec	Half-time, ($t_{\frac{1}{2}}$), sec
20	1.1	0.0008
80	18	0.014
200	80	0.045
500	270	0.15
1000	500	0.28

Drag Coefficients of Drops

The drag coefficient, C_D, is defined[7] as:

$$C_D = \frac{\text{Drag}}{(\text{Frontal Area})\left(\frac{\rho' v^2}{2g_c}\right)}$$

where g_c is as defined in the reference.

For steady motion of droplets, C_D becomes a function of Re alone, where

$$Re = \frac{dv\rho'}{\mu'}$$

d being the diameter of a sphere of volume equal to the drop, and ρ' and μ' being the density and viscosity of the air.

For droplets moving with streamline Stokesian motion, the expression for drag coefficient is extremely simple:

$$C_D = \frac{24}{Re} \qquad \text{(streamline motion)}.$$

However, for intermediate motion, and for turbulent Newtonian motion, the expression for drag is a more complex function of Reynolds number.

Hughes and Gilliland[7] recently published an excellent review of the motion of drops in which they summarized the available data on drag coefficients.

Figure 5 shows the drag coefficients for spheres and drops as a function of Re from 10 to 10,000.

Hughes and Gilliland point out that the analysis of the motion is greatly complicated by the period of acceleration and by the fluid nature of the drop. The two conventional methods for determining drag coefficient are (1) direct determination of drag in a wind tunnel, and (2) the measurement of terminal velocities of falling bodies. Because such measurements are made under conditions of steady flow, the important effect of accelerational drag, which generally exists, is not included.

Distortion of Drops

As shown in Figure 5, the drag coefficient for fluid drops is not the same as the drag for solid spheres, at the higher velocities, owing to distortion of the drop. Distortions are of two basic types: (1) those of an equilibrium nature, and (2) those of an oscillating nature resulting from vibrations about the equilibrium position. Distortion occurs because the pressure exerted by the surrounding fluid on a moving sphere is not uniform. However, the theoretical calculation of the shape of the drop is not possible because the pressure on the surface, which in turn depends on the shape of the drop, is not known exactly, even for a sphere.

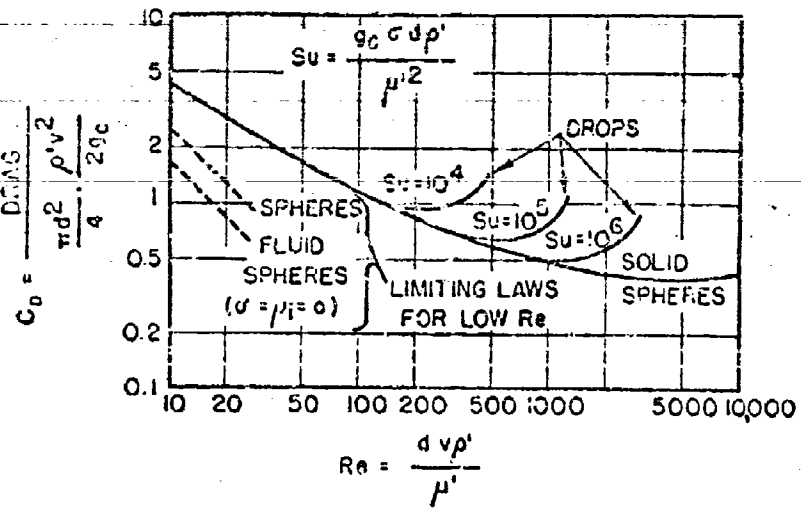

FIGURE 5. DRAG COEFFICIENTS OF SPHERES AND DROPS

(Hughes and Gilliland)[7]

Initial Velocity Of Droplets Leaving Centrifugal Spray Nozzles

A factor of practical interest in the dynamics of sprays is the initial velocity of the droplets as they leave the nozzle. Novikov[9] made a theoretical study of the velocity of liquid as it passes through the swirl chamber of a centrifugal atomizing nozzle. By a consideration of Bernoulli's equation and of the continuity equation, Novikov was able to develop expressions for the velocity and the thickness of the film of liquid issuing from the centrifugal-type nozzle.

Giffen and Muraszew[10] made a stroboscopic study of the discharge velocity of a centrifugal nozzle with an orifice diameter of 0.0429 inch. The initial discharge velocity of the fuel spray increased from 43 ft per sec at 100 psi to 68 ft per sec at 300 psi. The penetration distance was about 27 inches at both pressures.

Dynamic Effect Of Droplets Upon Each Other

Finally, mention should be made of the fact that the dynamic behavior of droplets may be influenced by the proximity of adjacent droplets. If the void fraction of the spray is 85 per cent or less, the Stokes' velocity is reduced by more than 50 per cent[11]. However, this effect of other nearby droplets is negligible when the per cent of voids is greater than 95, as is true a short distance from the nozzle orifice.

Therefore, in a fuel spray, the effect of surrounding droplets upon the behavior of any single droplet need be considered only as the liquid first emerges from the atomizer. A few centimeters from the nozzle, the concentration of droplets is so dilute that each droplet may be considered to behave independently of the other droplets in the spray.

Summary of Dynamics of Droplets

The movement of an individual droplet issuing from a spray nozzle depends upon the initial velocity of the drop and the drag due to the surrounding air. Drag coefficients of reasonable accuracy are available in the literature; however, the analysis of the motion is greatly complicated by the period of acceleration and by the distortion of the drop.

Additional experimental data, especially high-speed photography of droplets ejected at high velocities, are required for a better knowledge of the dynamic behavior of droplets. The spinning-disk atomizer is suggested as an excellent tool for use in studying the trajectory and velocity of droplets.

JMF/lq

REFERENCES

1. Jones, J. R., "Methods of Atomizing Liquid Fuels", J. of the Inst. of Petroleum, Vol. 39, No. 350, pp. 57-81, (Feb., 1953).

2. May, K. R., "The Cascade Impactor", J. of Sci. Instr. (London), Vol. 22, October, 1945, pp. 187-195.

3. Gaudin, A. M., "Principles of Mineral Dressing", Chapt. 5, The Movement of Solids in Fluids, McGraw-Hill Book Co., (1939).

4. Dallavalle, J. M., "Micromeritics", (Second Edition) Chapt. 2, Dynamics of Small Particles, Pitman Publishing Corp., (1948).

5. Davies, C. N., "The Sedimentation of Small Suspended Particles", Symposium on Particle Size Analysis, The Inst. of Chem. Engrs. and Society of Chemical Industry, London, Feb. 4, 1947.

6. Gumz, W., "Gas Producers and Blast Furnaces", John Wiley and Sons, (1950), p. 284.

7. Hughes, R. R. and Gilliland, E. R., "The Mechanics of Drops", Chem. Eng. Prog., Vol. 48, p. 497, (October, 1952).

8. Kumm, E. L., "Calculations on the Evaporation Rate of Sprays in Rapidly Moving Gas Streams", Report AL-916, June 23, 1949, North American Aviation, Inc., Aerophysics Laboratory, Project MX-770, RESTRICTED.

9. Novikov, I. I., "Atomization of Liquids by Centrifugal Nozzles", The Engineers' Digest, Vol. 10, No. 3, (March, 1949), p. 72.

10. Giffen, E. and Muraszew, A., "Fuel Injection in Internal-Combustion Engines, Atomization of Low-Pressure Fuel Sprays", The Motor Ind. Res. Assoc., Report No. 1948/5, Brentford, Middlesex.

11. Burgers, J. M., "The Effect of Concentration on the Speed of Sedimentation of Suspensions, Especially Suspensions of Spherical Particles", Proc. Acad. Sci., Amsterdam, Vol. 45, 1942, pp. 9-16, 126-7.

SQUID CONFERENCE ON ATOMIZATION, SPRAYS, AND DROPLETS
Northwestern Technological Institute
September 24-25, 1953

Appendix Number 2

(Paper Number 4 In Toto)

DROP-SIZE DISTRIBUTIONS AND THEIR AVERAGES

by

Ralph E. Thomas

Battelle Memorial Institute

September 1953

DROP-SIZE DISTRIBUTIONS AND THEIR AVERAGES

by

Ralph E. Thomas

WEIGHTED DISTRIBUTIONS AND WEIGHTED AVERAGES

In the current literature there are several types of distributions which are of importance in describing the size consist of sprays. These distributions arise naturally in the course of experimental investigations employing different techniques. For example, microscopic examination usually leads to droplet-size distributions by frequency or number; sedimentation and impaction lead to volume (or weight) distributions; and light extinction leads to surface distributions. In actual practice the true surface distribution and true volume distribution are seldom employed. Instead, the surface-weighed size distribution and volume-weighed size distributions are more frequently encountered. With the weighted distributions the x-axis is always measured in terms of droplet size so that one can transform from surface-weighted distribution to volume-weighted distribution, for example, without transforming the x-axis from surface to volume units. Mathematically, the surface-weighted size distribution may be written in terms of the surface increments over each size range. Thus, if $f_n(x)dx$ denotes the number of droplets in the range x to $x + dx$, then the corresponding increment of surface is given by

$$dS(x) = \frac{x^2 f_n(x)\, dx}{\int_0^\infty x^2 f_n(x)\, dx}$$

and the cumulative distribution function of the surface-weighted size distribution is given by

$$S(x) = \int_{-\infty}^{x} dS(t)$$

Similar expressions may be obtained for the volume-weighted size distribution.

Table I gives the cumulative distribution functions for the various weighted and unweighted distributions usually encountered in droplet statistics. Both the continuous and discrete forms are given.

Most of the averages and mean droplet diameters currently employed in droplet statistics are readily obtained by computing the moments of the various weighted size distributions. For example, the first moment of the surface-weighted size distribution is given by the expression,

$$\int_{-\infty}^{\infty} t(t^2 f_p(t)dt) \Big/ \int_{-\infty}^{\infty} t^2 f_n(t)dt$$

or in discrete terms by

$$\frac{\sum_{i=1}^{\infty} x_i (x_i^2 f_n(x_i)\Delta x_i)}{\sum_{i=1}^{\infty} x_i^2 f_n(x_i)\Delta x_i}$$

and this value is often called the Sauter, or "volume-surface" mean-droplet size. In a similar manner, the first moment of the volume-weighted size distribution may be computed. This value is usually called the weight-weighted mean diameter. From the mathematical expressions it is clear that the various moments of the weighted size distribution are expressible in terms of the moments of the unweighted size distribution. Thus, the Sauter mean diameter

TABLE 1. WEIGHTED AND UNWEIGHTED CUMULATIVE DISTRIBUTION FUNCTIONS EMPLOYED IN DROPLET STATISTICS

Cumulative function	Continuous form*	Discrete form**
Unweighted size distribution	$F_n(x) = \dfrac{\int_{-\infty}^{x} f_n(t)dt}{\int_{-\infty}^{\infty} f_n(t)dt}$	$F_n(x_k) = \dfrac{\sum_{i=1}^{k} f_n(x_i)\Delta x_i}{\sum_{i=1}^{N} f_n(x_i)\Delta x_i}$
Length-weighted size distribution	$F_l(x) = \dfrac{\int_{-\infty}^{x} t f_n(t)dt}{\int_{-\infty}^{\infty} t f_n(t)dt}$	$F_l(x_k) = \dfrac{\sum_{i=1}^{k} x_i f_n(x_i)\Delta x_i}{\sum_{i=1}^{N} x_i f_n(x_i)\Delta x_i}$
Surface-weighted size distribution	$F_s(x) = \dfrac{\int_{-\infty}^{x} t^2 f_n(t)dt}{\int_{-\infty}^{\infty} t^2 f_n(t)dt}$	$F_s(x_k) = \dfrac{\sum_{i=1}^{k} x_i^2 f_n(x_i)\Delta x_i}{\sum_{i=1}^{N} x_i^2 f_n(x_i)\Delta x_i}$
Volume-weighted size distribution	$F_v(x) = \dfrac{\int_{-\infty}^{x} t^3 f_n(t)dt}{\int_{-\infty}^{\infty} t^3 f_n(t)dt}$	$F_v(x_k) = \dfrac{\sum_{i=1}^{k} x_i^3 f_n(x_i)\Delta x_i}{\sum_{i=1}^{N} x_i^3 f_n(x_i)\Delta x_i}$

* In these equations $f_n(t)dt$ denotes the number of droplets in the size range t to $t + dt$.

** In these equations $f_n(x_i)\Delta x_i$ denotes the number of droplets in the size range given by Δx_i.

may be written as the first moment of the surface-weighted size distribution or as the ratio between the third and second moments of the unweighted size distribution. As a consequence of Cauchy's inequality,

$$\left(\sum_i a_i b_i\right)^2 \leq \left(\sum_i a_i^2\right)\left(\sum_i b_i^2\right) ,$$

it follows that the various moments of the size distribution are non-decreasing as the order of the moment increases. Thus, the arithmetic mean of the unweighted size distribution is less than, or equal to, the arithmetic mean of the length-weighted size distribution, which in turn is less than, or equal to, the arithmetic mean of the surface-weighted size distribution, etc. The more the droplet sizes are dispersed, the stronger the inequalities will be between the various moments. For this reason, the ratio of some higher-order moment to a lower-order moment is often taken as a measure of the dispersion of the droplet sizes. For example, the ratio of the weight-weighted mean drop size to the volume-surface mean drop size minus one is called the coefficient of variation of the surface-weighted size distribution. In a similar manner one may calculate the coefficients of variation corresponding to the unweighted, length-weighted, and volume-weighted distributions.

The variance of each of the weighted distributions may also be expressed in terms of the various moments. For example, the variance of the surface-weighted size distribution is equal to the product of the third and second moments of the unweighted size distribution minus the square of the second moment of the unweighted distribution.

Many of these equalities have proved important in experimental investigations involving surface-volume relations. Of particular interest is the fact that specific surface is inversely proportional to first moment of

the surface-weighted size distribution, and this moment, in turn, is equal to the harmonic mean of the volume-weighted size distribution. The fact that the volume-surface mean diameter is greater than the arithmetic mean of the unweighted size distribution and at the same time is less than the arithmetic mean of the volume-weighted distribution accounts for much of the acceptance of this average in droplet statistics.

Other averages of importance arise from the following type of consideration. Calculate the diameter of a hypothetical droplet whose surface area is equal to the total surface area of the spray divided by the total number of droplets in the spray. This is another kind of surface average and is easily shown to be equal to the geometric mean of the means of the length-weighted and unweighted size distributions. Averages of this type can always be reduced to a geometric mean of a set of moments of the various weighted size distributions.

Table 2 summarizes the formulas for the various averages usually encountered in droplet statistics.

SPECIFIC DISTRIBUTIONS FREQUENTLY EMPLOYED IN DROPLET STATISTICS

Normal Distribution

If the diameters of the droplets in a spray have a probability density function given by

$$y_n(x) = \frac{1}{\sigma_n \sqrt{2\pi}} \, e^{-\frac{(x-\mu'_{1,n})^2}{2\sigma_n^2}} \qquad -\infty < x < \infty ,$$

then the droplet sizes are said to be normally distributed. Although the normal distribution is extremely basic to most phases of statistical analysis,

TABLE 2. FORMULAS OF IMPORTANCE IN DROPLET STATISTICS

I ARITHMETIC MEANS

Arithmetic Mean of Unweighted Size Distribution

For continuous distribution: $$\mu_1', n = \frac{\int_{-\infty}^{\infty} x\, f_n(x)\,dx}{\int_{-\infty}^{\infty} f_n(x)\,dx}$$

For discrete distribution: $$\bar{x}_n = \frac{\sum_{i=1}^{\infty} x_i f_n(x_i)\Delta x_i}{\sum_{i=1}^{\infty} f_n(x_i)\Delta x_i}$$

μ_1' is the first moment of the continuous size distribution.

$\bar{x}_n$ is the first moment of the discrete size distribution.

$\bar{x}_n$ is called the mean diameter.

Arithmetic Mean of Length-Weighted Size Distribution

For continuous distribution: $$\mu_1', 1 = \frac{\int_{-\infty}^{\infty} x\,(x f_n(x)\,dx)}{\int_{-\infty}^{\infty} x f_n(x)\,dx}$$

For discrete distribution: $$\bar{x}_1 = \frac{\sum_{i=1}^{\infty} x_i (x_i f_n(x_i)\Delta x_i)}{\sum_{i=1}^{\infty} x_i f_n(x_i)\Delta x_i}$$

$\mu_1', 1$ is the first moment of the continuous length-weighted size distribution.

$\bar{x}_1$ is the first moment of the discrete length-weighted size distribution.

$\bar{x}_1$ is called the length-weighted mean diameter.

TABLE 2. FORMULAS OF IMPORTANCE IN DROPLET STATISTICS (Continued)

Arithmetic Mean of Surface-Weighted Size Distribution

For continuous distribution: $$\mu_{1,s}' = \frac{\int_{-\infty}^{\infty} x(x^2 f_n(x)dx)}{\int_{-\infty}^{\infty} x^2 f_n(x)dx}$$

For discrete distribution: $$\bar{x}_s = \frac{\sum_{i=1}^{\infty} x_i(x_i^2 f_n(x_i)\Delta x_i)}{\sum_{i=1}^{\infty} x_i^2 f_n(x_i)\Delta x_i}$$

$\mu_{1,s}'$ is the first moment of the continuous surface-weighted size distribution.
$\bar{x}_s$ is the first moment of the discrete surface-weighted size distribution.
$\bar{x}_s$ is called the Sauter or volume-surface mean diameter.

Arithmetic Mean of Volume- (or Weight-) Weighted Size Distribution

For continuous distribution: $$\mu_{1,v}' = \frac{\int_{-\infty}^{\infty} x(x^3 f_n(x)dx)}{\int_{-\infty}^{\infty} x^3 f_n(x)dx}$$

For discrete distribution: $$\bar{x}_v = \frac{\sum_{i=1}^{\infty} x_i(x_i^3 f_n(x_i)\Delta x_i)}{\sum_{i=1}^{\infty} x_i^3 f_n(x)\Delta x_i}$$

$\mu_{1,v}'$ is the first moment of a continuous volume-weighted size distribution.
$\bar{x}_v$ is the first moment of a discrete volume-weighted size distribution.
$\bar{x}_v$ is called the weight-weighted mean diameter.

II BASIC INEQUALITIES AMONG THE VARIOUS ARITHMETIC MEANS EMPLOYED IN DROPLET STATISTICS

For continuous distributions: $\mu_{1,n}' \leq \mu_{1,l}' \leq \mu_{1,s}' \leq \mu_{1,v}'$

For discrete distributions: $\bar{x}_n \leq \bar{x}_l \leq \bar{x}_s \leq \bar{x}_v$

TABLE 2. FORMULAS OF IMPORTANCE IN DROPLET STATISTICS (Continued)

III. FORMULAS FOR THE VARIANCE OF DROPLET SIZE DISTRIBUTIONS

Unweighted Size Distribution

For continuous distribution: $$\sigma_n^2 = \frac{\int_{-\infty}^{\infty} (x - \mu_1', n)^2 f_n(x)\,dx}{\int_{-\infty}^{\infty} f_n(x)\,dx}$$

For discrete distribution: $$s_n^2 = \frac{\sum_{i=1}^{\infty} (x_i - \bar{x}_n)^2 f_n(x_i)\Delta x_i}{\sum_{i=1}^{\infty} f_n(x_i)\Delta x_i}$$

Length-Weighted Size Distribution

For continuous distribution: $$\sigma_1^2 = \frac{\int_{-\infty}^{\infty} (x - \mu_1', 1)^2 x\, f_n(x)\,dx}{\int_{-\infty}^{\infty} x\, f_n(x)\,dx}$$

For discrete distribution: $$s_1^2 = \frac{\sum_{i=1}^{\infty} (x_i - \bar{x}_1)^2 x_i f_n(x_i)\Delta x_i}{\sum_{i=1}^{\infty} x_i f_n(x_i)\Delta x_i}$$

Surface-Weighted Size Distribution

For continuous distribution: $$\sigma_s^2 = \frac{\int_{-\infty}^{\infty} (x - \mu_1', s)^2 x^2 f_n(x)\,dx}{\int_{-\infty}^{\infty} x^2 f_n(x)\,dx}$$

For discrete distribution: $$s_s^2 = \frac{\sum_{i=1}^{\infty} (x_i - \bar{x}_s)^2 x_i^2 f_n(x_i)\Delta x_i}{\sum_{i=1}^{\infty} x_i^2 f_n(x_i)\Delta x_i}$$

TABLE 2. FORMULAS OF IMPORTANCE IN DROPLET STATISTICS (Continued)

Volume-Weighted Size Distribution

For continuous distribution: $$\sigma_v^2 = \frac{\int_{-\infty}^{\infty} (x - \mu_1',_v)^2 x^3 f_n(x)\,dx}{\int_{-\infty}^{\infty} x^3 f_n(x)\,dx}$$

For discrete distribution: $$s_v^2 = \frac{\sum_{i=1}^{\infty} (x_i - \bar{x}_v)^2 x_i^3 f_n(x_i)\Delta x_i}{\sum_{i=1}^{\infty} x_i^3 f_n(x_i)\Delta x_i}$$

IV FORMULAS SHOWING RELATIONS BETWEEN VARIANCES AND ARITHMETIC MEANS OF SIZE DISTRIBUTIONS

For continuous distributions:

$$\sigma_n^2 = (\mu_1',_1)(\mu_1',_n) - (\mu_1',_n)^2$$
$$\sigma_1^2 = (\mu_1',_s)(\mu_1',_1) - (\mu_1',_1)^2$$
$$\sigma_s^2 = (\mu_1',_v)(\mu_1',_s) - (\mu_1',_s)^2$$
$$\sigma_v^2 = (\mu_2',_v)(\mu_1',_v) - (\mu_1',_v)^2 \quad *$$

For discrete distributions:

$$s_n^2 = \bar{x}_1\bar{x}_n - (\bar{x}_n)^2$$
$$s_1^2 = \bar{x}_s\bar{x}_1 - (\bar{x}_1)^2$$
$$s_v^2 = \bar{x}_u\bar{x}_v - (\bar{x}_v)^2 \quad **$$

* In this equation $\mu_2',_v$ denotes the second moment of the continuous volume-weighted size distribution. Thus

$$\mu_2',_v = \frac{\int_{-\infty}^{\infty} x^2 (x^3 f_n(x)\,dx)}{\int_{-\infty}^{\infty} x^3 f_n(x)\,dx}$$

** In this equation $\bar{x}_u$ denotes the second moment of the discrete

TABLE 2. FORMULAS OF IMPORTANCE IN DROPLET STATISTICS (Continued)

volume-weighted size distribution. Thus

$$\bar{x}_u = \frac{\sum_{i=1}^{m} x_i^2 (x_i^3 f_n(x_i)\Delta x_i)}{\sum_{i=1}^{\infty} x_i^3 f_n(x_i)\Delta x_i}$$

V FORMULAS FOR THE COEFFICIENT OF VARIATION OF THE VARIOUS SIZE DISTRIBUTIONS ENCOUNTERED IN DROPLET STATISTICS

For continuous distributions:

$$\nu_n^2 = \frac{\sigma_n^2}{(\mu_1', n)^2} = \frac{(\mu_1', 1)}{(\mu_1', n)} - 1$$

$$\nu_s^2 = \frac{\sigma_s^2}{(\mu_1', c)^2} = \frac{(\mu_1', v)}{(\mu_1', s)} - 1$$

$$\nu_v^2 = \frac{\sigma_v^2}{(\mu_1', v)^2} = \frac{(\mu_2', v)}{(\mu_1', v)} - 1 \quad *$$

For discrete distributions:

$$V_n^2 = \frac{s_n^2}{(\bar{x}_n)^2} = \frac{\bar{x}_1}{\bar{x}_n} - 1$$

$$V_s^2 = \frac{s_s^2}{(\bar{x}_s)^2} = \frac{\bar{x}_y}{\bar{x}_s} - 1$$

$$V_v^2 = \frac{s_v^2}{(\bar{x}_v)^2} = \frac{\bar{x}_u}{\bar{x}_v} - 1 \quad **$$

* In this equation μ_2', v denotes the second moment of the continuous volume-weighted size distribution.

** In this equation $\bar{x}_u$ denotes the second moment of the discrete volume-weighted size distribution.

TABLE 2. FORMULAS OF IMPORTANCE IN DROPLET STATISTICS (Continued)

VI FORMULAS FOR THE GEOMETRIC MEANS OF THE VARIOUS SIZE DISTRIBUTIONS ENCOUNTERED IN DROPLET STATISTICS

For unweighted size distribution:

$$\bar{x}_n' = \left[\prod_{i=1}^{\infty} x_i^{\, f_n(x_i)\Delta x_i} \right]^{1 \Big/ \sum_{i=1}^{\infty} f_n(x_i)\Delta x_i}$$

For length-weighted size distribution: *

$$\bar{x}_l' = \left[\prod_{i=1}^{\infty} x_i^{\, a x_i f_n(x_i)\Delta x_i} \right]^{1 \Big/ \sum_{i=1}^{\infty} a x_i f_n(x_i)\Delta x_i}$$

For surface-weighted size distribution: *

$$\bar{x}_s' = \left[\prod_{i=1}^{\infty} x_i^{\, a x_i^2 f_n(x_i)\Delta x_i} \right]^{1 \Big/ \sum_{i=1}^{\infty} a x_i^2 f_n(x_i)\Delta x_i}$$

For volume-weighted size distribution: *

$$\bar{x}_v' = \left[\prod_{i=1}^{\infty} x_i^{\, a x_i^3 f_n(x_i)\Delta x_i} \right]^{1 \Big/ \sum_{i=1}^{\infty} a x_i^3 f_n(x_i)\Delta x_i}$$

* In these formulas a denotes a shape factor.

VII FORMULAS FOR THE HARMONIC MEANS OF THE VARIOUS SIZE DISTRIBUTIONS ENCOUNTERED IN DROPLET STATISTICS

For unweighted size distribution:

$$\bar{x}_n'' = \frac{\sum_{i=1}^{\infty} f_n(x_i)\Delta x_i}{\sum_{i=1}^{\infty} \frac{1}{x_i} f_n(x_i)\Delta x_i}$$

TABLE 2. FORMULAS OF IMPORTANCE IN DROPLET STATISTICS (Continued)

VII FORMULAS FOR THE HARMONIC MEANS OF THE VARIOUS SIZE DISTRIBUTIONS ENCOUNTERED IN DROPLET STATISTICS

For length-weighted size distribution:

$$\bar{x}_1'' = \frac{\sum_{i=1}^{\infty} x_i f_n(x_i)\Delta x_i}{\sum_{i=1}^{\infty} f_n(x_i)\Delta x_i} = \bar{x}_n$$

For surface-weighted size distribution:

$$\bar{x}_s'' = \frac{\sum_{i=1}^{\infty} x_i^2 f_n(x_i)\Delta x_i}{\sum_{i=1}^{\infty} x_i f_n(x_i)\Delta x_i} = \bar{x}_1$$

For volume-weighted size distribution:

$$\bar{x}_v'' = \frac{\sum_{i=1}^{\infty} x_i^3 f_n(x_i)\Delta x_i}{\sum_{i=1}^{\infty} x_i^2 f_n(x)\Delta x_i} = \bar{x}_s$$

VIII RELATIONS AMONG ARITHMETIC, GEOMETRIC, AND HARMONIC MEANS OF VARIOUS SIZE DISTRIBUTIONS

General Relation

Harmonic Mean $\leq$ Geometric Mean $\leq$ Arithmetic Mean

Unweighted size distribution: $\bar{x}_n'' \leq \bar{x}_n' \leq \bar{x}_n$

Length-weighted size distribution: $\bar{x}_1'' \leq \bar{x}_1' \leq \bar{x}_1$

Surface-weighted size distribution: $\bar{x}_s'' \leq \bar{x}_s' \leq \bar{x}_s$

TABLE 2. FORMULAS OF IMPORTANCE IN DROPLET STATISTICS (Continued)

VIII RELATIONS AMONG ARITHMETIC, GEOMETRIC, AND HARMONIC MEANS OF VARIOUS SIZE DISTRIBUTIONS

General Relation

Volume-weighted size distribution: $\bar{x}_v'' \leq \bar{x}_v' \leq \bar{x}_v$

Mixed inequality:

$$\bar{x}_n'' \leq \bar{x}_n' \leq \bar{x}_n = \bar{x}_1'' \leq \bar{x}_1' \leq \bar{x}_1 = \bar{x}_s'' \leq \bar{x}_s' \leq \bar{x}_s = \bar{x}_v'' \leq \bar{x}_v' \leq \bar{x}_v$$

$\bar{x}_s$ is called the volume-surface mean diameter.

$\bar{x}_v$ is called the weight-weighted mean diameter.

IX GEOMETRIC AVERAGES ENCOUNTERED IN DROPLET STATISTICS

The diameter of the droplet whose surface is equal to the total surface of the spray divided by the total number of droplets in the spray is given by

$$\bar{x}_s' = \sqrt{\bar{x}_n \bar{x}_1}$$

The diameter of the droplet whose volume is equal to the total volume of the spray divided by the total number of droplets in the spray is given by

$$\bar{x}_v' = \sqrt[3]{\bar{x}_n \bar{x}_1 \bar{x}_s}$$

it has not proved satisfactory in the representation of droplet sizes, except in instances where the droplets are produced by condensation, precipitation, or by chemical processes. Theoretically, the droplet sizes would be expected to tend to be normally distributed, provided the resultant drop size is the cumulative result of a very large number of very small chance influences where the influences act independently of each other and each contributes the same increment to the resulting drop size. Since most observed droplet disbributions are non-normal, it may be concluded that the underlying hypotheses are violated.

The fact that the normal distribution is fundamental to statistical inference while the normal distribution is relatively unimportant in droplet statistics may suggest that statistical inference may not be valid in the realm of droplet statistics. However, this is definitely not true. If an investigator finds that his data are normally distributed, he may apply the methods of statistical inference directly; if he finds that his data are non-normal, then the data may usually be transformed into a normal form. Although the unweighted droplet size distribution is non-normal, it may happen that the surface-weighted, or volume-weighted distribution may be regarded as normal.

Table 3 shows the form of various normal size distributions encountered in droplet statistics.

Log-Normal Distribution

In many instances, a non-normal droplet-size distribution can be transformed into a normal distribution by replacing the droplet diameter

TABLE 3. VARIOUS FORMS OF THE NORMAL SIZE DISTRIBUTION ENCOUNTERED IN DROPLET STATISTICS

I. If the unweighted droplet size is normally distributed, then

$$y_n(x) = \frac{1}{\sigma_n\sqrt{2\pi}}\, e^{-\frac{(x-\mu_1',_n)^2}{2\sigma_n^2}}, \quad -\infty < x < \infty$$

with an arithmetic mean equal to $\mu_1',_n$ and variance equal to σ_n^2.

II. If the surface-weighted droplet size is normally distributed, then

$$y_s(x) = \frac{1}{\sigma_s\sqrt{2\pi}}\, e^{-\frac{(x-\mu_1',_s)^2}{2\sigma_s^2}}, \quad -\infty < x < \infty$$

with mean equal to $\mu_1',_s$ and variance equal to σ_s^2.

III. If the volume-weighted droplet size is normally distributed, then

$$y_v(x) = \frac{1}{\sigma_v\sqrt{2\pi}}\, e^{-\frac{(x-\mu_1',_v)^2}{2\sigma_v^2}}, \quad -\infty < x < \infty$$

with mean equal to $\mu_1',_v$ and variance equal to σ_v^2.

with the logarithm of the droplet diameter. In this case the droplet size is said to follow a log-normal distribution given by

$$y_n(x) = \frac{1}{x\sqrt{2\pi}\,\sigma_{\log x}} e^{-\frac{(\log x - \log \bar{x}_n')^2}{\sigma^2_{\log x}}}, \quad x > 0$$

where $\log \bar{x}_n'$ denotes the logarithm of the arithmetic mean of $\log x$, and $\sigma^2_{\log x}$ denotes the variance of $\log x$.

Theoretically, the log-normal distribution can be deduced by assuming that droplet size is the result of a large number of small, independent impulses where the effect of each impulse is proportional to the size of the droplet. On this basis alone, it seems clear that the log-normal distribution would find wider applicability in droplet statistics than the normal distribution.

Table 4 shows the form of the various log-normal distributions encountered in droplet statistics.

Rosin-Rammler Distribution

The Rosin-Rammler distribution is a weight-weighted size distribution that has been successfully applied to size consists resulting from grinding. Mathematically, the probability density function is given by

$$y_w(x) = nbx^{n-1} e^{-bx^n}, \quad x > 0,$$

where n and b are numerical parameters. The parameter n is a characteristic of the substance of which the particles are composed; the value of b increases with increasing fineness. The weight-weighted mean particle size

TABLE 4. VARIOUS FORMS OF THE LOG-NORMAL DISTRIBUTION ENCOUNTERED IN FOREST STATISTICS

I. Unweighted log-normal:

$$y_n(x) = \frac{1}{x\sqrt{2\pi}\sigma_{\log x}} \cdot e^{-\frac{(\log x - \log \bar{x}_n')^2}{2\sigma_{\log x}^2}}, \quad x > 0$$

where $$\log \bar{x}_n' = \int_0^\infty (\log x)(f_n(x)dx)$$

$$\sigma_{\log x}^2 = \int_0^\infty (\log x - \log \bar{x}_n')^2 f_n(x)dx$$

II. Length-weighted log-normal:

$$y_l(x) = \frac{1}{x\sqrt{2\pi}\sigma_{\log x}} \cdot e^{-\frac{(\log x - \log \bar{x}_l')^2}{2\sigma_{\log x}^2}}, \quad x > 0$$

where $$\log \bar{x}_l' = \int_0^\infty (\log x) a x f_n(x)dx$$

$$\sigma_{\log x}^2 = \int_0^\infty (\log x - \log \bar{x}_l')^2 a x f_n(x)dx \ *$$

III. Surface-weighted log normal distribution:

$$y_s(x) = \frac{1}{x\sqrt{2\pi}\sigma_{\log x}} \cdot e^{-\frac{(\log x - \log \bar{x}_s')^2}{2\sigma_{\log x}^2}}, \quad x > 0$$

where $$\log \bar{x}_s' = \int_0^\infty (\log x) a x^2 f_n(x)dx$$

$$\sigma_{\log x}^2 = \int_0^\infty (\log x - \log \bar{x}_s')^2 a x^2 f_n(x)dx \ *$$

* In these formulas a denotes an appropriate shape factor.

TABLE 1. VARIOUS FORMS OF THE LOG-NORMAL DISTRIBUTION ENCOUNTERED IN DROPLET STATISTICS (Continued)

IV. Volume-weighted log normal distribution:

$$y_v(x) = \frac{1}{x\sqrt{2\pi}\sigma_{\log x}} e^{-\frac{(\log x - \log \bar{x}_v')^2}{2\sigma_{\log x}^2}}, \quad x > 0$$

where

$$\log \bar{x}_v' = \int_0^\infty (\log x)\, ax^3 f_n(x)\,dx$$

$$\sigma_{\log x}^2 = \int_0^\infty (\log x - \log \bar{x}_v')^2\, ax^3 f_n(x)\,dx \;*$$

* In these formulas a denotes an appropriate shape factor.

is easily found to be equal to $1/n\sqrt{b}\,\Gamma(1/n + 1)$, where $\Gamma(1/n + 1)$ represents the generalized factorial. From this it is clear that the greater the fineness of the consist, the smaller the weight-weighted mean diameter. The Rosin-Rammler distribution can be often fitted to data that are too skewed to be fitted by a log-normal distribution.

Table 5 shows the various forms of the Rosin-Rammler distribution.

Nukiyama-Tanasawa Distribution

In correlating the data obtained from air atomization of liquids, Nukiyama and Tanasawa used the following unweighted size distribution:

$$y_n(x) = \frac{b^3}{2!}\, x^2\, e^{-bx} \quad , x > 0 \quad .$$

This equation is one member of a family of statistical functions known as the Gamma distributions.

Table 6 shows the various forms of the Nukiyama-Tanasawa Distribution.

Other Distributions

In many instances the preceding size distributions will not yield an adequate fit to the observed data so that other distributions must be considered. Important alternative distributions include the following:

(1) Weibull's Volume-Weighted Size Distribution is given by

$$y_n(x) = \frac{n}{\bar{x}_v}\left(\frac{x - x_o}{\bar{x}_v}\right)^{n-1} e^{-\left(\frac{x - x_o}{\bar{x}_v}\right)^n} \quad ,$$

TABLE 5. VARIOUS FORMS OF THE ROSIN-RAMMLER DISTRIBUTION

I. Weight-weighted size distribution:

$$y_w(x) = n\,b\,x^{n-1}\,e^{-b\,x^n} \quad , x > o$$

Weight-weighted mean droplet size = $b^{-1/n}\,\Gamma(1 + 1/n)$

II. Surface-weighted size distribution *

$$y_s(x) = a\,n\,b\,x^{n-2}\,e^{-b\,x^n} \quad , x > o$$

Surface-weighted mean droplet size = a

III. Unweighted size distribution *

$$y_n(x) = a\,n\,b\,x^{n-4}\,e^{-b\,x^n} \quad , x > o$$

Mean droplet diameter = $a\,b^{2/n}\,\Gamma\,(1 - 2/n)$

* In these equations a denotes a shape factor.

TABLE 6. VARIOUS FORMS OF THE NUKIYAMA-TANASAWA DISTRIBUTION

I. Unweighted size distribution:

$$y_n(x) = \frac{b^3}{2!} x^2 e^{-bx} \quad , \; x > 0$$

Unweighted mean diameter: $3/b$

II. Surface-weighted size distribution:*

$$y_s(x) = \frac{ab^3}{2!} x^4 e^{-bx} \quad , \; x > 0$$

Surface-weighted mean diameter: $5!a/2b^3$

III. Volume-weighted size distribution:*

$$y_v(x) = \frac{ab^3}{2!} x^5 e^{-bx} \quad , \; x > 0$$

Volume-weighted mean diameter: $6!a/2b^4$

* In these formulas a denotes a shape factor.

where x_o is the smallest observed droplet size. This distribution has properties similar to those of the Rosin-Rammler distribution.

(2) The Gram-Charlier Series represents an arbitrary droplet-size distribution as an infinite series expansion in terms of the Hermite polynomials as follows:

$$y(x) = \sum_{k=0}^{\infty} a_k \, \phi^{(k)}(x) \quad ,$$

where

$$a_k = k! \int_{\infty}^{\infty} H_n(x) \, y(x) \, dx \quad ;$$

$\phi^{(k)}(x)$ denotes the k^{th} derivative of the error function, and $H_n(x)$ denotes the Hermite polynomial of degree n. For data which are approximately normal, the first few terms of the series expansion are usually sufficient.

(3) The Gamma Distributions are given by

$$y(x) = \frac{1}{\Gamma(\alpha + 1) \, \beta^{\alpha+1}} \, x^{\alpha} \, e^{-x/\beta} \quad , \quad x > 0 \quad .$$

The Nukiyama-Tanasawa distribution is a particular member of the family of Gamma distributions.

(4) Any non-negative function which has a finite integral over the range considered may serve as a size-distribution function. However, to enable one to make statistical inferences the parameters of the chosen distribution must have known statistical distributions. A distribution which gives an excellent fit may not be satisfactory for the purposes of statistical inference if the parameters do not have known distributions. For this reason, considerable care must be exercised in employing the various curve-fitting techniques which introduce new parameters into the distribution.

THE CHI-SQUARE TEST OF SIGNIFICANCE

Having chosen a particular type of distribution function, the constant parameters may be computed so that the curve gives the best fit to the data. Graphical analysis is often helpful in determining the order of magnitude of the parameters. The usual curve-fitting methods, such as least squares, are generally sufficient for this purpose. However, analytical methods should supplement the graphical methods in the final determination of the values of the parameters.

Having chosen the particular distribution function, the investigator should test the distribution against the observed data to determine whether the deviations between them can be attributed to chance. To accomplish this the following expression is computed:

$$\chi^2 = \Sigma \frac{(\text{expected value} - \text{observed value})^2}{\text{expected value}}$$

This gives the observed value of Chi-Square. If this value is very large, it is extremely improbable that the observed droplets originated in a spray having the size distribution being tested. In order to make the test quantitative, a level of significance is chosen, say α, and the corresponding χ^2_α is obtained from the χ^2 tables. Then, if the observed value of χ^2 exceeds the value of χ^2_α, the null hypothesis is rejected, and another type of distribution should be considered.

It may be noted that since the curve giving the best fit from a probability point of view is that curve which renders the value of χ^2 a minimum. This principle may be employed to compute the numerical values of parameters to be used in the distribution.

It should also be noted that the theoretical distribution may fit the data too well. In this instance the observed X^2 has a value so small that the probability of obtaining such a value is very close to zero. This result often occurs when too many parameters have been introduced into the distribution function. In general, the more parameters one has at his disposal, the better the distribution will fit the data. By eliminating a parameter, an overfitted distribution may be rendered less exact and a more reasonable value of X^2 may be obtained.

If the observed value of X^2 has a probability of occurrence between 0.05 and 0.95, it is usually agreed that the distribution being considered will serve as a basis for correlating the droplet-size data. In some instances, more than one distribution may give a satisfactory fit. In these instances, the distribution with the most reasonable physical interpretation should be given preference.

Inadequacy Of Relative Error

A simple calculation will show that the customary use of relative error* as a measure of the difference between theoretical and observed results is not adequate when probability considerations are involved. If the probability of obtaining a droplet in a specified size range is denoted by p, and if a sample of size n is drawn from the population, the expected number of droplets in the given range is equal to np. In general, the observed number of droplets will be different from the expected number. The observed number may be written as np', where p' denotes the empirical

* Relative error is defined as: $\frac{\text{Theoretical value} - \text{Observed value}}{\text{Theoretical value}}$

probability of obtaining a droplet in the given range. The relative error between the observed and expected results is given by

$$\frac{np' - np}{np} = \frac{p' - p}{p} ,$$

and this expression is independent of the size of sample. The contribution to χ^2 because of the difference between the observed and expected results is equal to

$$\frac{(np' - np)^2}{np} = \frac{n(p' - p)^2}{p} ,$$

and this value is directly proportional to the size of the sample. Thus, doubling the sample size doubles the value of χ^2 whenever the relative error remains constant. Consequently, the probability of obtaining the same relative error in a doubled size of sample is reduced. This is in accord with the intuitive notion that in larger samples the deviations due to chance should "settle down", and so oppose a constant relative error.

Limitations Of Statistical Analysis

Statistical analysis is most powerful when dealing with chance errors. In many instances, however, the errors may be systematic, and systematic errors do not have statistical populations. If, for example, droplet counts are made consistently too high, or weight measurements are made consistently too low, the resulting bias in the sample cannot be attributed to chance influences. In this instance statistical tests of

significance become meaningless, and the investigator may argue that his problem is thereby reduced to one of simple curve fitting where no regard need be given to probability considerations. However, it should be emphasized that unless the systematic errors can be determined and their effects eliminated, the fundamental problem of droplet statistics can not be solved. That is, the investigator will not be able to state the drop-size distribution of the spray from which the sample was drawn. If he contends that systematic errors cannot be eliminated, then he must admit that the parent drop-size distribution is both unknown and unknowable. On the other hand, if the systematic errors can be evaluated and eliminated, then a complete statistical analysis should produce a distribution which describes the parent droplet population with a specified degree of reliability.

RET:es

SQUID CONFERENCE ON ATOMIZATION, SPRAYS, AND DROPLETS
Northwestern Technological Institute
September 24-25, 1953

Appendix Number 3

(Paper Number 5 In Toto)

REVIEW OF MASS AND ENERGY TRANSFER BETWEEN LIQUID DROPLETS AND SURROUNDING GASES

by

Charles C. Graves
and
D. W. Bahr

National Advisory Committee for Aeronautics

Cleveland, Ohio

September 1953

REVIEW OF MASS AND ENERGY TRANSFER BETWEEN LIQUID DROPLETS AND SURROUNDING GASES*

By Charles C. Graves and D. W. Bahr

National Advisory Committee for Aeronautics
Cleveland, Ohio

Formulation of design criteria for high performance jet engine combustors or for industrial equipment such as spray dryers and cooling towers requires accurate knowledge of liquid vaporization rates. Conditions for evaporation vary widely among these various commercial and military applications. As an example, contrast the relatively low gas velocities in the cooling tower with velocities up to 400 feet per second in the ramjet. Or, contrast the relatively low temperatures in the cooling tower with conditions in the turbojet combustor where fuel is sprayed into regions approaching stoichiometric flame temperature. Accordingly, as shown on the first slide, this paper is concerned with conditions for single drops ranging from evaporation in low temperature quiescent surroundings on through to a discussion of the effects of forced convection on heat and mass transfer and, finally, to the consideration of the unsteady state process existing during the initial period of evaporation. Since another review paper will be presented on spray drying, the final portion of this paper will be limited to but a brief discussion of the evaporation of sprays.

First, let us consider the case of steady state drop evaporation in quiescent surroundings. This case is of interest since it offers a simple illustration of the principles involved in evaporation over the range of conditions covered in this paper. In addition, the calculated evaporation rates may be used as reasonable first estimates of evaporation rates for some applications.

The assumed physical model is shown on the next slide. Vapor, at the saturation pressure for the drop surface temperature, diffuses to the surrounding atmosphere. The drop surface temperature is maintained at a temperature sufficiently below that of the surroundings to provide the vaporization heat transfer requirements. We see then that the drop evaporation rate can be expressed in terms of either mass or heat transfer equations.

In the derivation of these equations it is assumed that a quasi-stationary state exists such that the vapor concentration and temperature

---

*Presented at Conference on Atomization, Sprays, and Droplets at Northwestern University, September 24-25, 1953.

gradients around the drop are, at every instant, those corresponding to equilibrium values for the existing drop size. It is also assumed that the temperature in the drop interior is constant at its equilibrium value. For the condition of spherical symmetry, the differential heat and mass transfer equations for a spherical surface a distance r from the drop center are given by equations (1) and (2). In equation (1) the term $c_p \frac{T_s - T_\infty}{}$ is the enthalpy change of the fuel vapor between the drop surface and the surface considered, L is the latent heat of vaporization at the surface temperature, and dw/dt is the drop evaporation rate. This equation simply equates the heat transferred by mass movement of the diffusing vapor to that transferred by thermal conductivity. Equation (2) is the application of the Stefan diffusion equation (ref. 1) to drop evaporation.

For evaporation in quiescent surroundings these equations are integrated between the drop surface and infinity to obtain equations (3) and (4). For these integrations, c_p, k, and D/T were taken as constants and represent mean values between the drop surface and the surroundings. Vapor pressure in the surrounding atmosphere was assumed negligible. Predicted drop evaporation rates would be obtained from simultaneous solution of these heat and mass transfer equations along with the assumption that the vapor pressure at the drop surface corresponds to saturation pressure for the drop surface temperature.

For evaporation in low temperature surroundings the sensible heat change of the vapor between the drop surface and surroundings is small compared to the latent heat of vaporization. Consequently, equation (3) reduces to equation (5) on the next slide. This equation is similar in form to that of simple heat transfer to a sphere in quiescent surroundings. Similarly, for evaporation where the vapor pressure at the drop surface is small compared to the total pressure, equation (4) reduces to equation (6), the Langmuir equation (ref. 2). It is seen that equations (5) and (6) are of similar form, illustrating the widely known analogy between heat and mass transfer. On the other hand, as was seen from equations (3) and (4) on the previous slide, the analogy breaks down for evaporation in high temperature surroundings. In either case, however, drop evaporation is proportional to drop diameter.

Equation (6) has been verified for evaporation of small drops in room air by the work of Topley and Whytlaw-Gray (ref. 3); Houghton (ref. 4); and Whytlaw-Gray and Patterson (ref. 5).

We have seen that equation (6) applies only when the surface vapor pressure is small compared with the total pressure. Consider for a moment that other corrections might be made to equation (6). If we divide this equation by drop surface area, we see that the evaporation rate per unit surface area is inversely proportional to drop diameter. In addition, this rate is inversely proportional to total pressure as determined by the pressure dependency of the diffusion coefficient. Consequently, as we

approach sufficiently small drops and total pressures, the evaporation rate per unit area as obtained from equation (6) could exceed the theoretical maximum evaporation rate for evaporation in a vacuum as obtained from gas kinetics (ref. 6). This theoretical maximum evaporation rate for a drop evaporating isothermally in a vacuum is given by equation (7) where is 1/4 the arithmetic mean molecular velocity and α is the evaporation or accomodation coefficient.

The case of evaporation of very small drops was treated theoretically by Fuchs (ref. 7). He considered diffusion to start, not at the drop surface, but at a distance approximately one mean free path from the drop surface. The mass transfer drop evaporation equation according to this picture is given by equation (8). Here Δ is the distance between the drop surface and the surface where the diffusion process is assumed to start. For drop diameters large compared to Δ, this equation reduces to the Langmuir equation. For very small drops, the second term in the denominator approaches zero and the evaporation rate approaches that of a drop evaporating in a vacuum as given by equation (7). Similarly, for the larger size drops, this theoretical maximum evaporation rate is approached as we go to sufficiently low pressures where Δ is again large compared to the drop diameter. The Fuchs theory was confirmed experimentally by the work of Bradley and his co-workers (refs. 8, 9, and 10).

For most applications, the correction according to the Fuchs theory is mainly of academic interest. The effect generally becomes noticeable at atmospheric pressures only when we reach drop sizes in the order of one micron. Similarly, correction for the effect of surface tension on surface saturation vapor pressure generally becomes noticeable only for drops smaller than one micron. Finally, Lochak and Langstroth (ref. 11) have shown that errors resulting from the assumption of quasi-stationary state are negligible under most circumstances.

Now let us consider the case of evaporation in high temperature quiescent surroundings. There has been little experimental work done for this region. All of this work appears to have been done for the case of single drops burning in quiescent atmospheres. Since drop burning has been treated theoretically as a special case of drop evaporation, a brief discussion of the work is warranted. For the high temperature evaporation case of burning drops we use the heat transfer equation and avoid use of the mass transfer equation for fuel vapor by assuming the surface temperature to be the fuel boiling point. Since we are dealing with large temperature differences, the error involved in this assumption is minor. The next slide presents the model for the burning drop as proposed by Spalding (ref. 12). In this picture oxygen diffuses from the surrounding atmosphere C to a burning zone of negligible thickness located at B, while exhaust products diffuse in the opposite direction. Heat balance equations are set up for regions AB and BC. In addition, a mass transfer equation is set up for the diffusion of

oxygen from the surrounding atmosphere to the burning zone. The drop burning or evaporation rate is obtained from simultaneous solution of these equations This burning rate is given by equation (1), which represents the simplified equation where thermal conductivity and specific heats are considered to be constant Accordingly, these values are taken as mean values for the appropriate regions of integration. Equation (2) gives the simple heat transfer equation for low temperature evaporation. From comparison of these two equations, we can see that the term in the brackets of equation (1) represents an effective temperature difference for evaporation. It is noted that for this case of high temperature evaporation, the sensible heat change of the fuel vapor is large compared to the latent heat of vaporization. Consequently, serious error would result by neglecting the enthalpy of the fuel vapor. This is illustrated by the next slide. On the ordinate is plotted the ratio of evaporation rate predicted by the simple heat transfer equation to that predicted by the equation accounting for vapor enthalpy. Curves are presented for isooctane and water drops evaporating in quiescent surroundings at various temperatures. It is seen that at the higher temperatures, the simple heat transfer equation would predict much higher evaporation rates for the case of isooctane drops. This effect is much less pronounced for water which has a high latent heat of vaporization. Effects of diffusing vapor enthalpy changes on predicted evaporating rates were treated theoretically by Ackermann (ref. 13) and by Colburn and Drew (ref. 14).

Spalding (ref. 15) conducted some experimental work on a burning sphere. However, the sphere had a diameter of $1\frac{1}{2}$ inches and consequently was subject to considerable free convection effects which were difficult to predict. In addition, it is believed that possible high radiation heat transfer to the sphere may have obscured the results.

Godsave (ref. 16) determined the burning rates for a number of hydrocarbon fuels from photographic measurements of silhouettes of burning drops suspended in quiescent air. Initial drop diameters were approximately 1700 microns. An approximate relationship was found between burning rate and the enthalpy change between liquid fuel at the initial drop temperature and vapor fuel at the boiling point. Burning rate was directly proportional to drop diameter.

Godsave (ref. 17) also treated the burning of single drops theoretically by using the heat transfer equation for evaporation in high temperature surroundings. Predicted burning rates were obtained by assuming a temperature for the burning zone surrounding the drop and by substituting film thicknesses for the region between the drop surface and burning zone as determined from photographs. Good agreement between predicted and experimental values was obtained by this method.

Graves (ref. 18) used the Golsave procedure to determine the effect of oxygen concentration on the burning rate of single isooctane drops. Both the absolute burning rates and changes in burning rate with oxygen concentration were predicted rather closely by equations based on the Spalding theory.

Even for the relatively small drop sizes investigated by Golsave (ref. 16) and Graves (ref. 18), the free convection effects resulting from the high temperature gradients may have been appreciable. In their paper on drop evaporation, Ranz and Marshall (ref. 19) suggested a correlation for free convection similar in form to the forced convection correlation. If this relation is used in conjunction with a modified Grashof number (ref. 20) for the burning drops, we might expect buoyancy forces to increase burning rate in the order of 50 percent over that for an infinite film thickness. In view of the drop diameter dependency of the Grashof number drop burning rate would then be proportional to a power of diameter greater than unity. However, data for the burning drops did not appear to show this trend. Since the drops were initially at a temperature considerably below the equilibrium value, a possible factor offsetting the effect of free convection would be the unsteady state heating of the drop interior. This process will be considered later in the paper.

We have considered drops evaporating in quiescent surroundings. For negligible free convection effects the film thickness was considered to be infinite. For this case we also assumed spherical symmetry of the transfer paths. Now, let us consider drop evaporation under forced convection.

With forced convection we no longer have spherical symmetry. In fact there may be a large change in local transfer rate over the drop surface. An example of this change is shown in the next slide. Here local transfer rates, expressed as a fraction of the transfer rate at the forward stagnation point, is plotted against the angle from the forward stagnation point. The data were obtained by Frossling (ref. 21) for the sublimation of a naphthalene head. Boundary layer theory predicts that the local transfer rate should be a maximum at the forward stagnation point, decrease gradually to a minimum near the separation point and then rise gradually to a new maximum at the rear stagnation point. This type of change is seen to be followed in the figure.

Ranz and Marshall (ref. 19) determined the temperature profile around an evaporating water drop as shown in the next slide. It is seen that, for a Reynolds number of approximately 8, the boundary layer thickness and drop diameter are approximately the same. From the change in spacing of the lines of constant temperature difference it is also seen that there is again a gradual decrease in local transfer rate from the maximum value at the forward stagnation point.

Correlations of experimental data neglect changes in these local transfer rates and consider an average value for the entire sphere. The total drop in either temperature or partial pressure of diffusing vapor is assumed to take place across a stagnant film. Consequently, heat or mass transfer equations such as given in the first two slides are used but for a finite film thickness.

The heat and mass transfer equations for forced convection evaporation are shown on the next slide. It is seen that these equations are similar to those for evaporation in a quiescent atmosphere. The only difference is the use of a Nusselt number to account for the effect of forced convection on evaporation rate. For negligible forced convection the Nusselt numbers reduce to a limiting lower value of 2 and these equations become identical with those previously shown for evaporation in a quiescent atmosphere. It is noted that the heat transfer equation is of the simple form that neglects effects of enthalpy of the diffusing vapor on the calculated evaporation rate.

First, let us consider the question of heat transfer for spheres. Theoretical approaches to heat transfer for spheres have been made by Johnstone, Pigford, and Chapin (ref. 22); by Kudryashev (ref. 23); by Drake, Sauer, and Schaaf (ref. 24); and by Tang, Duncan, and Schweyer (ref. 25). Predicted values of average Nusselt number over the sphere for heat transfer in air are shown in the next figure.

Drake followed the assumptions of Johnstone, but used a different method for obtaining the solution to the Fourier-Poisson equation. For Reynolds numbers below 1000 the predicted values are above those of Johnstone. In this analysis radial velocity was assumed to be zero and tangential velocity was assumed everywhere to equal mean stream velocity. For Reynolds numbers approaching zero this assumed model gives a limiting Nusselt number of 2 as is required for heat transfer in quiescent surroundings. Kudryashev obtained an analytical solution based on the thermal boundary layer.

Another approach to the problem of heat transfer rates from spheres is the Reynolds analogy. This can be stated that, when heat and momentum are transferred in corresponding ways, the Nusselt number over the product of Reynolds and Prandtl numbers equals half the friction factor as determined from skin friction.

For system such as flat plates where skin friction is readily determined, the Reynolds analogy holds fairly well for Prandtl numbers close to unity. Chilton and Colburn (ref. 26) suggested simple modifications to the Reynolds analogy for Schmidt and Prandtl numbers other than unity. These are given by the familiar j-factors.

For the case of bluff bodies where it is difficult to separate skin friction from total drag, there has been little work done to determine the applicability of the analogy. However, work by Sherwood (ref. 27) on

cylinders and, more recently, work by Tang and Drake (ref. 25) on spheres indicate that the analogy holds fairly well for fluid bodies for Prandtl numbers close to unity. The Nusselt number based on the Reynolds analogy and calculated by Tang is also presented in this slide. It is noted that the friction factor in this calculation is based on the summation of local friction over the entire surface and not on the resultant of friction forces in the direction of the free stream.

Now let us consider empirical correlations for heat transfer for spheres. An extensive survey of published data on heat and mass transfer to spheres was conducted by Williams (ref. 28) in 1942. The suggested relation for Nusselt number for heat transfer is given by equation (1) of the next slide. In the range of lower Reynolds numbers (<1000) the data showed considerable scatter. This range of Reynolds numbers was investigated recently by Tang (ref. 25), who determined heat transfer rates for steel spheres in air streams. The conditions covered included sphere diameters from 1/8 to 5/8 inch, temperature differences between sphere and air streams from 8° to 100° F and Reynolds numbers from 50 to 2000. The correlation obtained in this investigation is given by equation (2).

Ranz and Marshall determined evaporation rates of suspended water and benzene drops. Reynolds numbers ranged from zero to approximately 200, drop diameters from 600 to 1100 microns, and air temperatures from room temperature to approximately 400° F. For evaporating water drops, the data were correlated by equation (3).

Ingebo (ref. 29) determined evaporation rates of nine pure liquids in air streams having temperatures ranging from approximately 80° to 1000° F. A liquid drop was simulated by means of a wetted cork sphere having an average diameter of 0.69 centimeter. Reynolds numbers ranged from 1200 to 5700. In a later report (ref. 30) data were obtained in air for static pressures from approximately 1/2 to 2 atmospheres. The majority of these later experiments were conducted at room temperature. In order to extend the correlation, an additional limited set of data were obtained for streams of helium, argon and carbon dioxide. The final correlation obtained by Ingebo (ref. 30) is given by equation (4). Here g is the gravitational constant, l is the mean free molecular path, and $\bar{c}$ the root mean square molecular velocity.

The next slide presents a comparison of the various predicted and experimental curves for heat transfer for spheres in air. Here Nusselt number is plotted against Reynolds numbers from 50 to 2000. In order to compare the Ranz and Marshall correlation with the other curves on the figure, the Prandtl number in this correlation is taken as that of dry air. The correlation obtained by Ingebo is based, among other factors, on a Schmidt number which varies with the liquid being vaporized. The Ingebo correlation was used in this figure by taking the Schmidt number and thermal conductivity ratio equal to unity. The correlation factor $gl/\bar{c}^2$ was calculated on the basis of air. The predicted curves of Drake and Tang are given in color.

It is seen that the data of Tang are more closely predicted by the Reynolds analogy than by the curve of Drake for the higher Reynolds number range. For the lower Reynolds number range there is good agreement between the predicted curve of Drake and the experimental curves of both Ranz and Ingebo. The predicted curve of Kudryashev is not shown on the figure. However, it lies below and approximately parallel to the experimental curve of Tang.

Now let us consider the treatment of forced convection evaporation in terms of the mass transfer equation. Little theoretical work has been done for forced convection evaporation specifically in terms of the mass transfer equation. However, in view of the analogy between heat and mass transfer for low temperature evaporation, the theoretical treatments for heat transfer could be applied to the mass transfer case.

A theoretical analysis for mass transfer to spheres was given by Johnstone and Kleinschmidt (ref. 31). They assumed the sphere contacts a cylindrical tube having an inner diameter equal to that of the sphere and a thickness equal to the distance a diffusing molecule could travel in the time the sphere moves one diameter. Increase in relative velocity between sphere and surrounding gases decreases available diffusion time and consequently the thickness of the imaginary tube. All molecules contained within the tube are considered to be absorbed.

Use of the diffusion equation in correlations of drop evaporation data is limited to evaporation in relatively low temperature surroundings since this equation becomes highly sensitive to experimental errors in drop surface temperature at the higher surface vapor pressures. Correlations of Nusselt number for mass transfer are shown in the next slide.

Williams correlated mass transfer data by Froessling; Johnstone and Williams (ref. 32); Powell (ref. 33); and McInness (ref. 34). The recommended equations in terms of the Nusselt number for mass transfer are given by equation (1).

Maisel and Sherwood (ref. 35) reported data on evaporation of water and benzene from porous spheres. The data for water were in good agreement with equation (1). Deviation of data for benzene from this equation was thought to be attributed to incomplete wetting of the sphere.

Froessling correlated data for room temperature evaporation of water, aniline, naphthalene and nitrobenzene for Reynolds numbers from 2.4 to 7[illegible]. The Froessling correlation is given by equation (2).

The Ranz and Marshall correlation for mass transfer is given by equation (3). This correlation is of same form as their heat transfer correlation, but where Prandtl number is replaced by Schmidt number as would be expected from the analogy between heat and mass transfer. The data of Froessling; Powell; and Maisel and Sherwood agree well with this correlation.

Kinzer and Gunn (ref. 36) obtained a predicted Nusselt number for mass transfer given by equation (4). The equation was applied to evaporation rate data obtained for water drops falling freely at their terminal velocities under room air conditions. Data were obtained for drop diameters from approximately 20 to 4200 microns. Application of the experimental data to equation (4) indicated that the term F in the equation varied from zero to a value greater than 2 in the low range of Reynolds numbers. For Reynolds numbers from approximately 100 to 2000, F had values close to unity.

It is seen that drop evaporation rates for forced convection have been correlated in terms of either the heat transfer or mass transfer equation. Use of either of these equations requires accurate knowledge of drop surface temperature. This temperature is given by the wet bulb temperature. For the special case of water evaporation, drop surface temperature may be taken as the adiabatic saturation temperature with little error. However, for other liquids, this assumption would result in serious error and wet bulb temperature must be used. Wet bulb temperatures may be calculated by simultaneous solution of the heat and mass transfer equations. For the case of evaporation of pure liquids in high temperature surroundings, Ingebo has obtained a correlation for wet bulb temperature in terms of the liquid boiling point.

The majority of the data have been obtained for pure liquids. However, Ranz and Marshall determined drop temperatures for water drops containing dissolved and suspended solids. For drops containing solids in solution, the initial evaporation rates were those to be expected for saturated solutions even though the average concentrations in the drops were below the saturation value. For drops containing solids in suspension, the initial drop evaporation rate was that corresponding to pure water.

There appear to be very little data published on evaporation of wide boiling range hydrocarbons. However, work is being conducted by Lamb and co-workers in this field.

The final case of single drop evaporation to be considered is that of unsteady state evaporation. Here the initial drop temperature is either above or below its equilibrium value and frequently changes with time. Both theoretical and experimental work has been reported for this case.

The analytical treatments generally assume either a finite thermal conductivity within the drop as given by that of the liquid or assume an infinite thermal conductivity. Circulation within the drop results in an effective thermal conductivity between these two values, the circulation effects being more pronounced for the larger drop sizes and Reynolds numbers (ref. 37).

Topps (ref. 38) studied evaporation rates of small drops falling through a high temperature atmosphere. Initial drop diameters ranged from

approximately 300 to 550 microns. His results for this rather narrow range of drop diameters indicated that the evaporation rate varied approximately as the drop diameter to the four and a half power. This is contrasted to the variation of evaporation rate with drop diameter to the two and a half power for steady state evaporation at the high Reynolds numbers. This large difference was attributed by Topps to unsteady state conduction of heat to the drop interior which reduced the heat available for evaporation of the smaller drops.

Godsave (ref. 39) investigated theoretically the unsteady state heating of burning drops of heavy fuel oil. He was primarily interested in effects of the unsteady state period on the formation of carbon residue. A finite thermal conductivity was assumed. For evaporation in high temperature atmospheres he concluded that the drop interior tended to remain below cracking temperature till the last stages of evaporation. For evaporation in lower temperature surroundings the drop interior tends to reach high temperatures in the early stages of evaporation with resultant increases in cracking and cenosphere formation.

Kinzer and Gunn (ref. 36) used an ingenious apparatus to determine the time rate of change in the average temperature of falling water drops. A simplified theoretical expression was obtained for the time required for the drops to reach 63 percent of the equilibrium temperature difference. The analysis assumed thermal conductivity of the drop interior to be infinite. Satisfactory agreement was found between the predicted and experimental value.

Recently El Wakil, Myers, and Uyehara (ref. 40) studied the unsteady state evaporation of pure liquid drops for conditions similar to those existing in jet engine combustors. In their analysis, thermal conductivity of the drop interior was also assumed to be infinite. Temperature-time, mass-time, and penetration-time histories were calculated for drops evaporating in air. This type of calculation involves a step by step trial and error procedure for simultaneous solution of the heat transfer, mass transfer, and drop motion equations.

A typical figure is shown in the next slide. Here percent evaporated, relative velocity, and drop temperature are plotted against time in milliseconds. The calculations are for an isooctane drop having an initial diameter of 50 microns, initial temperature of 50° F, and initial velocity relative to air of 100 feet per second. The air was assumed to be at a pressure of 1/2 atmosphere and temperature of 1000° F. For these conditions, the amount of heat going to the drop interior far exceeded that supplying latent heat of vaporization during the major portion of the unsteady state period. Calculations of this type indicate that at high air temperatures and for high volatility fuels, the unsteady state period may represent an appreciable part of the total vaporization time

We now come to the vaporization of liquid sprays. Since the subject of spray drying will be treated in another paper, this portion will be

limited to a brief discussion of data of more direct concern to the combustion chamber designer.

Extension of single drop data to sprays is difficult since both drop size distribution of the spray and relative velocities between the air and droplets must be known. In addition there are such complicating factors as drop distortion, unsteady state evaporation, and interaction between drops.

Several theoretical analyses of spray evaporation have been made by using single drop relations in conjunction with assumed drop size distributions. One such analysis is that described by Probert (ref. 41). In this treatment, all drops were assumed to have zero relative velocity with respect to the air. The spray was assumed to follow the Rosin-Rammler distribution equation. With this analysis, the fraction of unevaporated spray after a given period of time is given in terms of the spray drop size distribution constants and the evaporation rate for a single drop in a quiescent atmosphere.

Another theoretical treatment of spray vaporization has been presented by Tribus, Klein, and Rembowski (ref. 42). Zero relative velocity between the air and droplets was also assumed. It is shown that, given an initial drop-size spectrum, successive spectra may be deduced by calculating the variation in drop size of the largest drop and relating all other drop sizes to this maximum drop size.

Because of the lack of data on drop size distribution for a particular apparatus, it is generally difficult to apply evaporation rate relationships for single drop to sprays. Some attempts have been made to obtain direct measurements of spray vaporization rates in air streams. An investigation of this type has been described by Fledderman and Hanson (ref. 43). The influence of turbulence and air velocity on the spray vaporization rate was studied. A theoretical analysis of spray vaporization was also included in this study. In the analysis, Frocssling's equation for single droplet evaporation was combined with the drop size distribution equation of Nukiyama and Tanasawa (ref. 44).

The experimental measurements were obtained by sampling hexane sprays at various distances downstream of a hollow-cone spray nozzle. The percent of evaporated spray was determined over a limited range of air velocities. The results indicated a strong dependence of evaporation rate on the relative velocity. Increased turbulence intensity was also found to increase the spray vaporization rate. The test results, however, did not provide conclusive information on the effect of scale of turbulence on the evaporation rate.

The results of a few measurements of the evaporation rate of kerosene sprays in essentially still air have been reported by Sacks (ref. 45).

In this program, the kerosene was injected from a swirl chamber fuel nozzle at pressures of 50 and 80 psi. Over this range of conditions, from 0.2 to 0.3 percent of the spray was found to evaporate per second. This is contrasted to a calculated value of approximately 50 percent per second. These predicted values were obtained by using the Langmuir equation, Probert's relations, and drop size distribution values obtained from the Bowen and Joyce relations (ref. 46). This very large difference between predicted and experimental values was attributed primarily to the inability of the Langmuir equation to predict evaporation rates for single drops when in a cloud of drops.

A study of the effect of the air flow and fuel injection parameters on the evaporation of gasoline-type fuel sprays has recently been made by Bahr (ref. 47). This investigation was conducted over ranges of conditions common in ram-jet and afterburner engines. An empirical correlation was obtained for the evaporation over the range of conditions investigated. This study will be discussed by Mr. Bahr at the conclusion of this paper.

In summary, we find good agreement between predicted and experimental steady state evaporation rates of single drops in low temperature quiescent surroundings. Experimental data on evaporation in high temperature quiescent surroundings are limited to the case of burning drops. Again good agreement is found between experiment and theory.

Theoretical approaches to steady state evaporation under forced convection are far more difficult. Consequently, a number of simplifying assumptions have been required in order to obtain solutions. Agreement between theory and experiment is satisfactory in view of the approximations used in the theory. Semi-empirical correlations for steady state forced convection evaporation are available in terms of either the heat or mass transfer equations. Drop surface temperatures may be determined from simultaneous solution of these equations or obtained from a correlation in terms of the liquid boiling point for the higher temperature evaporation conditions.

The major portion of the experimental data was obtained for pure liquids. Some data were obtained on the effect of both dissolved and suspended solids on the evaporation rate of water drops. There appear to be very little data available at the present time that would permit predictions to be made for the evaporation rate of wide boiling range hydrocarbons.

Calculations have been made for the unsteady state period of drop evaporation. Some of these calculations indicate that unsteady state evaporation may represent an appreciable portion of the total drop evaporation time. However, there are very little experimental data available for this part of the vaporization process.

Several theoretical approaches have been made to the problem of predicting evaporation rates of liquid sprays. However, but a limited amount of experimental work has been done to determine how well data for single drops would apply to vaporization rates of sprays in air stream. This type of investigation would involve the difficult task of measuring simultaneously both drop size distribution and evaporation rate. One investigation indicated an appreciable difference between predicted and experimental spray evaporation rates in a low temperature low velocity air stream. An empirical correlation was obtained from direct measurements of evaporation of an isooctane spray in a high velocity air stream. Further experimental work of this type is needed to determine the effect of fuel properties and fuel injection systems on spray evaporation rates.

REFERENCES

1. Jakob, Max: Heat Transfer, Vol. 1, John Wiley & Sons, p. 601.

2. Langmuir, I.: "The Evaporation of Small Spheres," Phys. Rev., Vol. 12, 1918, p. 368.

3. Topley, B., and Whytlaw-Gray, R. W.: "Experiments on the Rate of Evaporation of Small Spheres as a Method of Determining Diffusion Coefficients," Phil. Mag., Vol. 4, 1927, pp. 873-888.

4. Houghton, H. G.: "A Study of the Evaporation of Small Water Drops," Physics , Vol. 4, 1933, pp. 419-424.

5. Whytlaw-Gray, R. W., and Patterson: Smoke, Arnold, London, 1932.

6. Kennard, E. H.: Kinetic Theory of Gases, McGraw-Hill, 1939, pp. 68-71.

7. Fuchs, N.: "Concerning the Velocity of Evaporation of Small Droplets in a Gas Atmosphere," NACA TN 1160, 1947.

8. Bradley, R. S., Evans, M. G., and Whytlaw-Gray, R. W.: "The Rate of Evaporation of Droplets. I - Evaporation and Diffusion Coefficients, and Vapour Pressures of Dibutyl Phthalate and Butyl Stearate," Proc. Roy. Soc. (London), Vol. 186, No. A1006, Ser. A, Sept. 1946, pp.368-390.

9. Birks, J., and Bradley, R. S.: "The Rate of Evaporation of Droplets. II - The Influence of Changes of Temperature of the Surrounding Gas on the Rate of Evaporation of Drops of Di-n-butyl Phthalate," Proc. Roy. Soc. (London), Vol. 198, No. A1053, Ser. A, Aug. 1949, pp. 226-239.

10. Bradley, R. S., and Shellard, A. D.: "The Rate of Evaporation of Droplets. III - Vapour Pressures and Rates of Evaporation of Straight-Chain Paraffin Hydrocarbons," Proc. Roy. Soc. (London), Vol. 198, No. A1053, Ser. A, Aug. 1949, pp. 239-251.

11. Luchak, G., and Langebroth, G. O.: "Applications of Diffusion Theory to Evaporation from Droplets and Flat Surfaces," Def. Res. Bd., Exp. Sta. Rep. 171, 1950.

12. Spalding, D. B.: "Combustion of Liquid Fuel in a Gas Stream - Part I," Fuel, Vol. 29, 1950, pp. 2-7.

13. Ackerman, G.: "Waermeuebergang und Molekulare Stoffuebertragung in Gleichenfeld bei Grossen Temperatur-und Partialdruckdifferenzen," Forschungsheft 382, Beilage 24, Forschung auf dem Gebiete des Ingenieurwesens. Ausgabe B Band 8, Januar/Februar, 1937.

14. Colburn, A. P., and Drew, T. B.: "The Condensation of Mixed Vapors," Trans. Am. Inst. of Chem. Engineers, Vol. 33, (1937) pp. 197-214.

15. Spalding, D. B.: "Combustion of Liquid Fuels in a Gas Stream," Fuel, Vol. 29, 1950, pp. 25-32.

16. Godsave, G. A. E.: "Burning of Single Drops of Fuel - Part II - Experimental Results," N. G. T. E. Rept., R. 87, 1951.

17. Godsave, G. A. E.: "Burning of Single Drops of Fuel - Part III - Comparison of Experimental and Theoretical Burning Rates and Discussion of the Mechanism of the Combustion Process," N. G. T. E. Rept., R. 68, 1952.

18. Graves, C. C.: "Combustion of Single Isooctane Drops in Various Quiescient Oxygen-Nitrogen Atmospheres," The Third Midwestern Conference on Fluid Mechanics, 1953, pp. 759-778.

19. Ranz, W. E., and Marshall, W. R.: "Evaporation from Drops - Parts I and II," Chem. Eng. Prog. Vol. 68, 1952, pp. 141-146, 173-180.

20. Spalding, D. B.: "The Combustion of Liquid Fuels," Fourth Symposium on Combustion, The Williams and Wilkins Co., (1953) PP. 847-864.

21. Frossling, N.: "Uber die Verdunstung fallender Tropfen," Gerl. Beitr. Geophys., Bd. 52, Heft. 1/2, 1939, pp. 170-216.

22. Johnstone, H. F., Pigford, R. D., and Chapin, J. H.: "Heat Transfer to Clouds of Falling Particles," Bull., No. 330 Eng. Exp. Station, Univ. of Illinois, Vol. 37, No. 43, June 17, 1941.

23. Kundryashev, L. I.: "A Refinement of the Calculation of the Heat Transfer Coefficient Between Gas and Suspendod Particles by Application of the Thermal Boundary-Layer Method," Translated by M. Goyer, Lib. Translation, No. 368, British R. A. E. (Farnborough) March, 1951.

24. Drake, R. M., Sauer, F. M., Jr., and Schaaf, S. A.: "Forced Convection Heat Transfer from Cylinders and Spheres in a Rarified Gas," Rep. No. HE-150-74, Contract No. N7-onr-295-Task 3, Inst. Eng. Res., Univ. of California, Nov. 15, 1950.

25. Tang, V. S., Duncan, J. M., and Schweyer, H. E.: "Heat and Momentum Transfer Between a Spherical Particle and Air Streams," NACA TN 2867, 1953.

26. Chilton, T. H., and Colburn, A. P.: "Mass Transfer Coefficients. Prediction from Data on Heat Transfer and Fluid Friction," Ind. Eng. Chem., Vol. 26, 1934, pp. 1183-7.

27. Sherwood, T. K.: "Heat Transfer, Mass Transfer, and Fluid Friction," Ind. and Eng. Chem., Vol. 62, No. 10, Oct. 1950, pp. 2077-2084.

28. Williams, G. C.: "Heat Transfer, Mass Transfer and Friction for Spheres," Sc. D. Thesis. M. I. T., 1942.

29. Ingebo, R. D.: "Vaporization Rates and Transfer Coefficients for Pure Liquid Drops," NACA TN 2368, 1951.

30. Ingebo, R. D.: "Study of Pressure Effects on Vaporization Rate of Drops in Gas Streams," NACA TN 2850, 1953.

31. Johnstone, H. F., and Kleinschmidt, R. V.: "The Absorption of Gases in Wet Cyclone Scrubbers," Trans. Am. Inst. Chem. Engrs., Vol. 34, 1938, pp. 181-198.

32. Johnstone, H. F., and Williams, G. C.: "Absorption of Gases by Liquid Droplets," Ind. Eng. Chem., Vol. 31, No. 8, 1939, pp. 993-1001.

33. Powell, R. W.: "Further Experiments on the Evaporation of Water From Saturated Surfaces," Trans. Inst. Chem. Engrs. (London), Vol. 18, 1940, p. 993.

34. MacInness, D. A.: "Heat Transfer, Mass Transfer and Friction for Spheres," Sc. D. Thesis, M. I. T., 1942.

35. Maisel, D. S., and Sherwood, T. K.: "Evaporation of Liquids into Turbulent Gas Streams," Chem. Eng. Prog., Vol. 46, No. 3, 1950, pp. 131-138.

36. Kinzer, G. D., and Gunn, R.: "The Evaporation Temperature and Thermal Relaxation Time of Freely Falling Water Drops," Journal of Meteorology, Vol. 8, No. 2, April, 1951.

37. Hughes, R. R., and Gilliland, E. R.: "The Mechanics of Drops," Chem. Eng. Prog., Vol. 48, No. 10, 1952, pp. 497-504. (Also unpublished experimental work of M. M. El Wakil, P. Myers, and O. E. Uyehara at Univ. of Wisconsin.)

38. Topps, J. E. C.: "An Experimental Study of the Evaporation and Combustion of Falling Droplets," N. G. T. E. Memo., No. M105, 1951.

39. Godsave, G. A. E.: "The Burning of Single Drops of Fuel - Part IV - The Flow of Heat and Carbon Residue Formation in Drops of Fuel," N. G. T. E. Rept., No. 4. 125, 1952.

40. El Wakil, M. M., Uyehara, O. A., and Myers, P. S.: Univ. of Wisconsin. (Unpublished Work.)

41. Probert, R. P.: "The Influence of Spray Particle Size and Distribution in the Combustion of Oil Droplets," Phil. Mag., Vol. 37, 1946, pp. 94-105.

42. Tribus, M., Klein, J. S., and Hembowski, J.: "A Method for Calculating the Rate of Evaporation and Change in Drop Size Distribution for Pure Sprays Injected into Unsaturated Air," Eng. Res. Inst., Univ. of Michigan, 1952. Prepared for Wright Air Development Center, U. S. Air Force Contract AF 18(600)-51, E.O. No. 462 Br-1.

43. Fledderman, R. G., and Hanson, A. R.: "The Effects of Turbulence and Wind Speed on the Rate of Evaporation of a Fuel Spray," Rept. No. CM667 Eng. Res. Inst., Univ. of Michigan, 1951. Prepared for U. S. Navy, Bur. Ord., Contract No. NOrd 7924. TASK UMH-3D.

44. Bevans, A. S.: "Mathematical Expressions for Drop Size Distribution in Sprays," presented at Conference on Fuel Sprays, Univ. of Michigan, 1949.

45. Sacks, W.: "The Rate of Evaporation of a Kerosine Spray," Nat. Aero. Est., Ottawa, Canada, Note 7, 1951.

46. Bowen, C. G., and Joyce, J. A.: "The Effects of Cone Angle, Pressure, and Flow Number on the Particle Size of a Pressure Jet Atomizer," Shell Pet. Ltd., Tech. Rept. No. I.C.T./17 March, 1948.

47. Bahr, D. W.: "Evaporation and Spreading of Isooctane Sprays in High Velocity Air Streams," Paper presented at Conference on Atomization, Sprays and Droplets, Northwestern Univ., Sept., 1953. NACA RM E53I14.

EVAPORATION OF SINGLE DROPS

1. QUIESCENT SURROUNDINGS
   - (a) LOW TEMPERATURE
   - (b) HIGH TEMPERATURE
2. FORCED CONVECTION
   - (a) HEAT TRANSFER
   - (b) MASS TRANSFER
3. UNSTEADY STATE

EVAPORATION OF SPRAYS

FIG. 1

EVAPORATION OF A SINGLE DROP

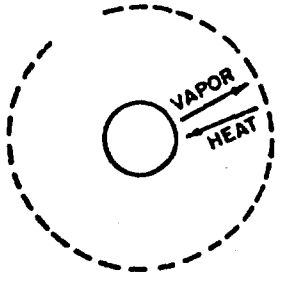

$$\left[c_p(T-T_0)+L\right]\frac{dw}{dt} = -KA\frac{dT}{dr} \qquad (1)$$

$$\frac{dw}{dt} = \frac{DPA}{R_vT}\frac{d}{dr}\left[\ln\left(1-\frac{p_v}{P}\right)\right] \qquad (2)$$

$$\frac{dw}{dt} = \frac{2\pi K}{c_p}\, d_0 \ln\left[1+c_p\frac{(T_\infty - T_0)}{L}\right] \qquad (3)$$

$$\frac{dw}{dt} = 2\pi\frac{DP}{R_vT}\, d_0 \ln\left[1-\frac{p_v}{P}\right] \qquad (4)$$

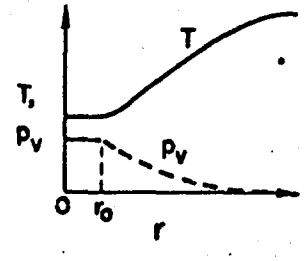

FIG. 2

EVAPORATION OF A SINGLE DROP

$$\frac{dw}{dt} = \frac{2\pi K d_o}{L} (T_\infty - T_o) \qquad (5)$$

$$\frac{dw}{dt} = \frac{2\pi D d_o}{R_v T} p_{v,o} \qquad (6)$$

$$\frac{dw}{dt} = \frac{\pi d_o^2 \nu a p_{v,o}}{R_v T} \qquad (7)$$

$$\frac{dw}{dt} = \frac{\frac{2\pi D d_o p_{v,o}}{R_v T}}{\frac{2D}{d_o \nu a} + \frac{d_o}{d_o + \Delta}} \qquad (8)$$

FIG. 3

BURNING OF SINGLE DROP

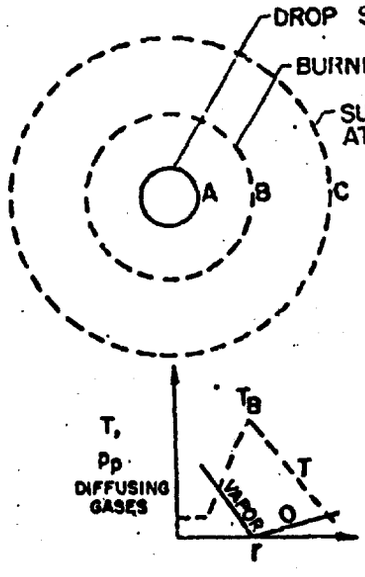

$$\frac{dw}{dt} = \frac{2\pi K d_o}{L} \left[\int_{T_A}^{T_B} \frac{L\, dT}{L + c_p (T - T_o)} + \int_{T_C}^{T_B} \frac{L\, dT}{Q + h_{o_2} - h_p} \right] \qquad (1)$$

$$\frac{dw}{dt} = \frac{2\pi K d_o}{L} (T_\infty - T_o) \qquad (2)$$

FIG. 4

EFFECT OF ENTHALPY CHANGE OF VAPOR ON PREDICTED EVAPORATION RATES OF WATER AND ISOOCTANE DROPS

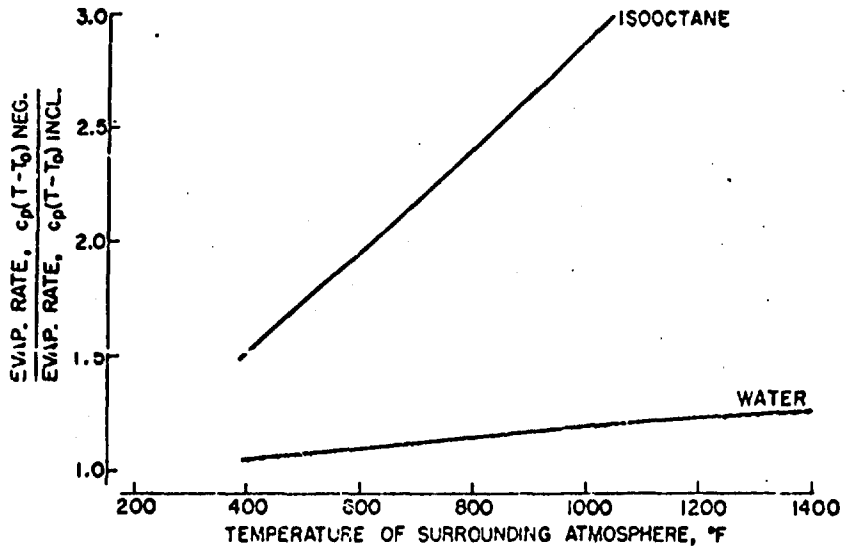

FIG. 5

CHANGE IN LOCAL TRANSFER RATE OVER SURFACE OF SPHERE

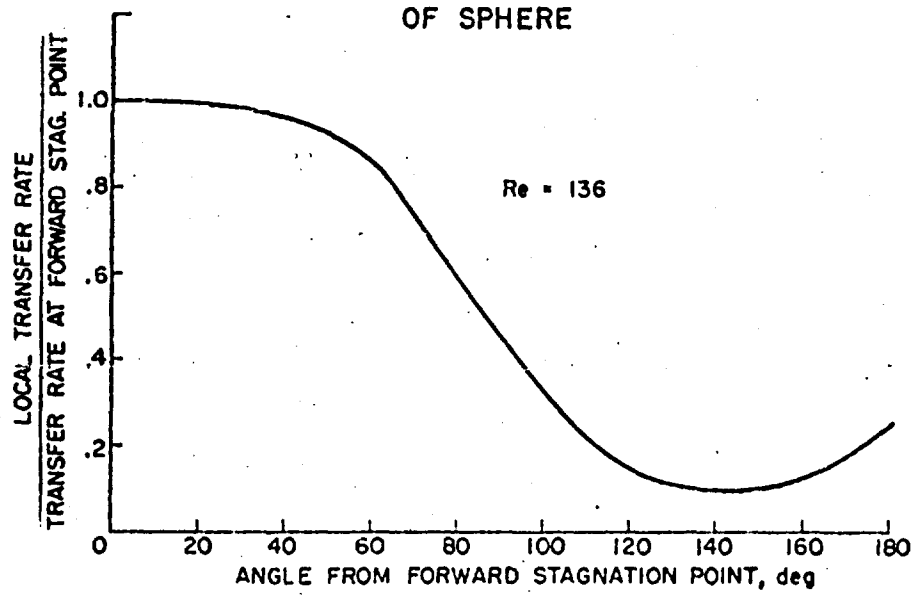

FIG. 6

TEMPERATURE EXPLORATION AROUND EVAPORATING WATER DROPLET

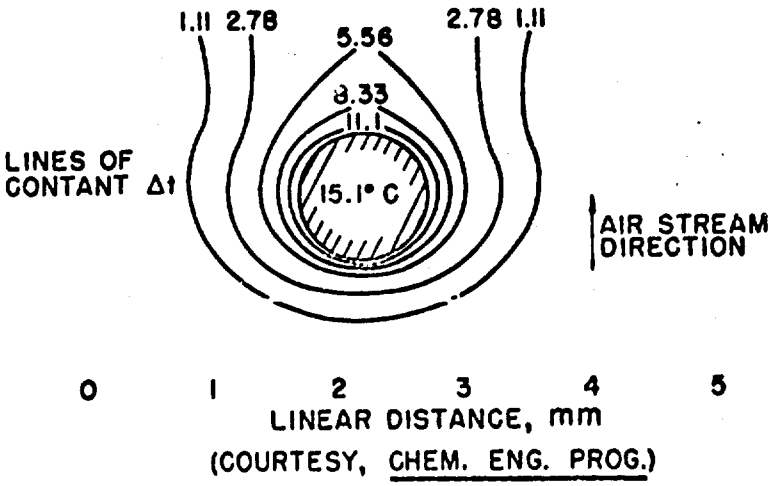

(COURTESY, CHEM. ENG. PROG.)

FIG. 7

FORCED-CONVECTION HEAT AND MASS TRANSFER EQUATION

$$\frac{dw}{dt} = Nu \frac{\pi K d_o}{L} (T_1 - T_o) \qquad \underline{\text{Heat}}$$

$$\frac{dw}{dt} = Nu' \frac{\pi D P d_o}{R_v T p_{B,M}} (p_{v,o} - p_{v,1}) \qquad \underline{\text{Mass}}$$

where

$p_{B,M}$ = log mean pressure of inert gas

FIG. 8

COMPARISON OF PREDICTED NUSSELT NUMBERS
HEAT TRANSFER FOR SPHERES

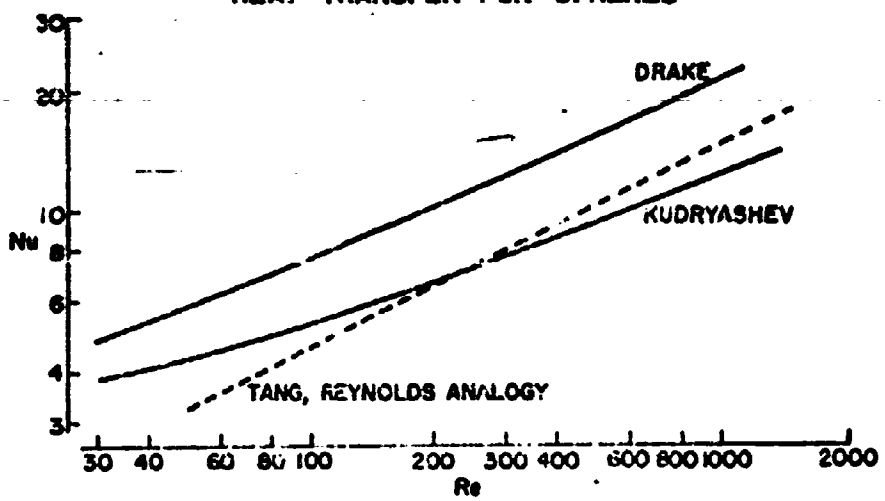

FIG. 9

EMPIRICAL CORRELATIONS OF HEAT-TRANSFER DATA FOR SPHERES

$$Nu = 0.37(Pr)^{1/3}\,(Re)^{0.6} \qquad (1)\ \text{WILLIAMS}$$

$$Nu = 2.1 + 0.37(Re)^{0.5} \qquad (2)\ \text{TANG}$$

$$Nu = 2.0 + 0.6(Pr)^{1/3}\,(Re)^{1/2} \qquad (3)\ \text{RANZ}$$

$$Nu = 2.0 + 2.58\times10^{6}\left[Re\ Sc\left(\frac{\rho_1}{\rho_2}\right)\right]^{0.6}\left(\frac{K_g}{K_v}\right)^{0.6} \qquad (4)\ \text{INGEBO}$$

FIG. 10

THEORETICAL AND EMPIRICAL NUSSELT NUMBER
HEAT TRANSFER FOR SPHERES IN AIR

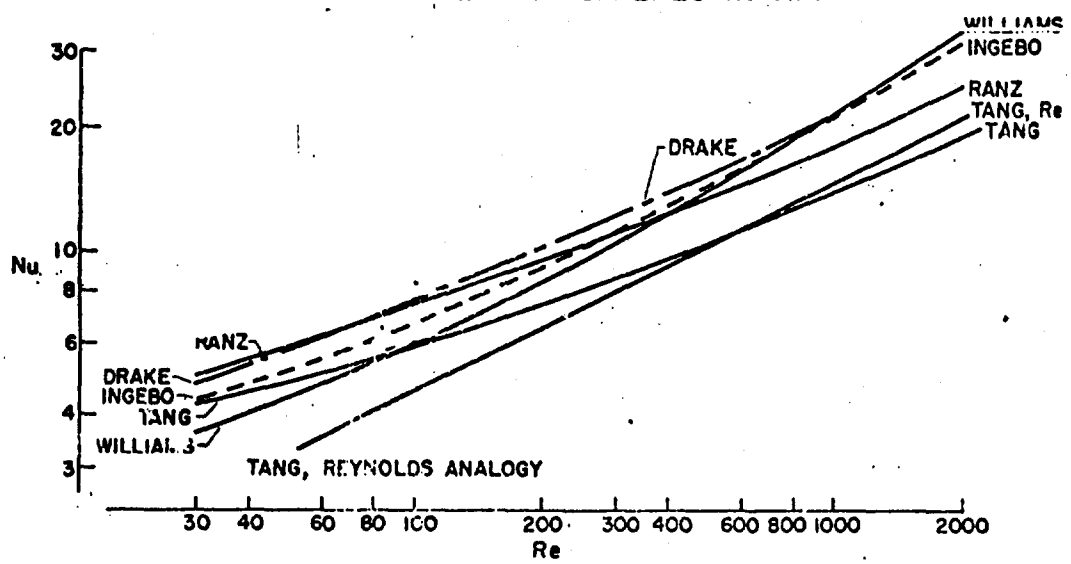

FIG. 11

EMPIRICAL CORRELATIONS FOR MASS TRANSFER FOR SPHERES

$$\left.\begin{aligned} Nu' &= 1.5\ Sc^{1/3}\ Re^{0.35} \qquad 5<Re<400 \\ Nu' &= 0.43\ Sc^{1/3}\ Re^{0.56} \qquad 400<Re<10 \end{aligned}\right\} \quad (1) \qquad \text{WILLIAMS}$$

$$Nu' = 2 + 0.55\ Sc^{1/3}\ Re^{1/2} \qquad (2) \qquad \text{FROESSLING}$$

$$Nu' = 2 + 0.60\ Sc^{1/3}\ Re^{1/2} \qquad (3) \qquad \text{RANZ}$$

$$Nu' = 2 + \frac{F}{4\pi}\ Sc^{1/2}\ Re^{1/2} \qquad (4) \qquad \text{KINZER}$$

FIG. 12

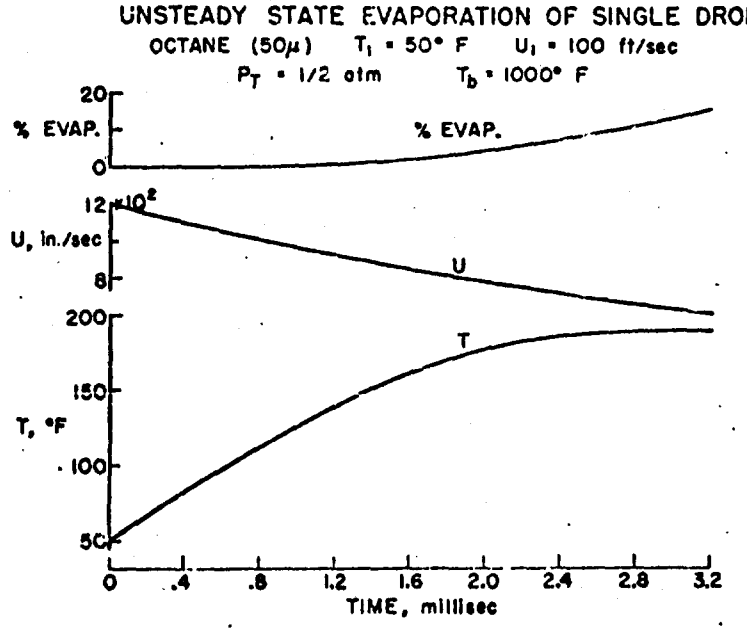

FIG. 13

SQUID CONFERENCE ON ATOMIZATION, SPRAYS, AND DROPLETS
Northwestern Technological Institute
September 24-25, 1953

Appendix Number 4

(Paper Number 12 In Toto)

INJECTION IN AFTERBURNING TURBOJETS

by

D. G. Samaras

Aeronautical Research Laboratory
Wright Air Development Center
Air Research and Development Command
Wright-Patterson Air Force Base

September 1953

INJECTION IN AFTERBURNING TURBOJETS

I Introduction

From the very beginning of Jet Propulsion the operational limitations of the simple turbojet were understood and discussed, and methods for improvement were suggested (Ref. 1).

Among others, these limitations in performance included the following:

a. Relatively long take-off runs;

b. Low initial rates of climb;

c. The requirement for better top speed performance (short duration).

Afterburning, as it was first introduced (Ref. 1), also included cooled compression in the compressor (e.g. by liquid injection in the inlet). This increases the thrust of the unit by increasing the temperature of the gases before expansion in the propelling nozzle and by decreasing the compression work in the compressor. Figure 1 shows this cycle. Considerable theoretical and experimental work was then performed in order to realize the above advantages.

It should be stressed here that, although considerable improvements can be obtained in the subsonic flight region by afterburning (Ref. 2), its employment at supersonic flight speeds has been found to be not only desirable but imperative (Ref. 3).

Although the idea of afterburning is simple, its full realization in an engine is fraught with a number of difficulties such as:

a. Stable operation at any altitude without screech;

b. Operation at high altitude without flame out;

c. Propelling nozzle cooling.

The first two difficulties are strongly influenced by the injection process of the fuel in the afterburner, and will be discussed in more detail.

Generally speaking, two extreme, although representative, operational cases of afterburners are apparent:

1. The afterburner operates only a comparatively short part of the total flight time;

2. The afterburner operates almost the whole flight time.

The operational requirements of the first case are as follows:

a. Short take-off run;

b. High rate of climb;

c. Short time of top thrust operation;

d. Long time economical cruising.

As the afterburning system will operate only during a short time interval it should be designed in such a way as to avoid large losses during the long non-afterburning time. In this case higher afterburner losses may be tolerated during the afterburning period.

The operational requirements of the second case are as follows:

a. Long time economical cruising with afterburning at high Mach speeds and altitudes;

b. Good take-off and transonic operation is desirable;

c. The operational altitude and speeds are well above those of the first case.

From the above it is obvious that the afterburning system should be designed so as to operate with minimum loss during cruising. In this case higher afterburner losses may be tolerated during the non-afterburning period.

The high altitudes and Mach speeds anticipated may put severe restrictions on the design.

The flame stability at cruising, and during the acceleration phases should have an amply safe range of operation; however, that may not be always feasible and flame out at altitude may become a serious problem.

II Types of Afterburning

It is well known (Ref. 4) that the combustion of a fuel in a propulsion system can be effected according to the following modes:

a. Injection of liquid fuel in a gas stream;

b. Injection of vaporized fuel in a gas stream;

c. Catalytic combustion on a suitable hot surface.

We shall discuss here only the mode of liquid injection. Afterburning types are sub-divided according to the position of the injection apparatus and the direction of injection relative to the gas stream.

According to the above, the following main types of afterburning may distinguish themselves:

a. Preturbine injection. This type has been investigated experimentally by the Air Force (Power Plant Laboratory, Wright Patterson Air Force Base) (Fig. 2-a.);

b. After turbine upstream injection with flame holder stabilization (Fig. 2-b);

c. After turbine upstream injection with flame in the trailing vortices of the turbine blades (Fig. 2-c.);

d. After turbine downstream injection with flame holder stabilization (Fig. 2-d);

e. After turbine downstream injection with tail-cone-end injector (Fig. 2-e.).

III Advantages and Disadvantages of the Different Types:

The first type, namely, preturbine injection, does not need a flame holder as the flame stabilization is mostly effected by the turbine blades. This type when properly designed, is accompanied by high combustion efficiency and a short length of propelling nozzle is always attained. The main disadvantage of this type is complete lack of control of the temperature distribution, which results in the appearance of hot spots but no combustion instabilities. Cooling of the fuel injectors may be necessary.

The second type of afterburner, when properly designed, gives high combustion efficiency and a satisfactory temperature distribution. A short length of propelling nozzle is always obtained. However, because of the presence of flame holders, choking of the flow in the flame holder region appears at high fuel-air ratios, accompanied by the deleterious oscillating phenomenon known as screech.

The third type seems to possess the best all-around characteristics, namely, high combustion efficiency and controllable temperature distribution. Since there are no flame holders, no flow blockage exists and consequently, it is quite free of screech. This type may need considerable cooling of the fuel injectors. The length of the propelling nozzle can be kept short.

The fourth type requires a comparatively longer length of afterburner to keep the combustion efficiency at a permissible level. This sometimes is accompanied by high pressure losses. Because flame holders are employed for flame stabilization, blocking of the flow occurs and this type is very susceptible to screech.

The fifth type is the oldest utilized experimentally. The combustion efficiency obtained in 1943 was around 60%. After the war, by the use of long propelling nozzles, the combustion efficiency was improved at the expense of high pressure losses. This type, when properly designed, is not susceptible to screech.

It is evident that the shorter the length of the propelling nozzle the easier the solution of the cooling problem.

Table I gives a summary of the above discussion:

TABLE I

Injection Type	Temperature Distribution	Combustion Efficiency	Pressure Losses	Screech	Propelling Nozzle
1	Bad	Good	Low	Free	Short
2	Good	Good	Low	Badly	Short
3	Good	Good	Low	Free	Short
4	May Be Good	Not So Good	High	Very Badly	Long
5	May Be Good	Poor	Not So High	May Be Free	Very Long

In the case where a part load operation is required, staggering of the injectors into two or three rows results in a satisfactory operation of the afterburner.

IV Injection, Evaporation and Ignition

The main objective of injection and ignition is to secure a uniform temperature and velocity distribution during and after combustion and also to give sufficient residence time to the fuel droplets so that the process of evaporation, mixing and ignition will have enough time to be effectively performed.

In order to provide a better design, quantitative data on the injection, evaporation, mixing, and ignition of fuel droplets are necessary. Ignition data are mostly concerned with spontaneous ignition.

The time and length of droplet penetration are important and can be calculated from known formulas both for single droplets and for simple, mathematical droplet distributions (sprays).

Upstream injection is not as sensitive to droplet size and distribution as is downstream injection. This results from the larger droplet having greater upstream penetration. Again greater penetration is accompanied by longer residence time. The opposite is true for downstream injection. Under similar flow conditions such as velocity, flame holder distribution, temperature, etc., the deterioration of altitude operation of an afterburner with downstream injection is more pronounced than that of one with upstream injection because of shorter residence time.

The variables appearing in the design of an afterburner are:

a. Temperature of the turbine outlet gases;

b. Pressure of the turbine outlet gases;

c. Oxygen depletion (vitiation) of the turbine outlet gases;

d. Fuel characteristics;

e. Fuel pressure;

f. Fuel droplet size and distribution.

Work performed by B.P. Mullins during the last decade at the N.G.T.E. indicates that the influence of the droplet size and the fuel characteristics (when kerosene type fuels are used), do not have a pronounced influence on the ignition lag. All other variables have a profound effect on the evaporation and ignition process.

Figure 3 shows the ignition lag of a standard fuel plotted as a function of gas pressure at constant gas temperatures. It is obvious that as the pressure decreases for a given gas temperature, the ignition lag increases rapidly, thus resulting in a rapid decrease of combustion efficiency with altitude. This may be remedied up to a certain degree by an increase of the turbine outlet gas temperature or an increase of the flame holder drag.

The above indicates quite clearly a ceiling in afterburner operation upon which the injection type has a profound effect. In spite of the above, it is encouraging that the introduction of turbine blade cooling results, to some extent, in higher turbine outlet temperatures and thus raises the operating ceiling of the afterburner by reducing the ignition lag.

Figure 4 shows the influence of vitiation (contamination with combustion gases). In this the ignition lag is plotted against the relative depletion of oxygen at constant gas temperatures. This figure indicates that when maintaining all other conditions constant, increasing the turbine outlet temperature will result in a higher degree of vitiation which will tend to decrease, somewhat, the advantages, shown in Figure 3, of an increase in temperature.

V Heat Addition; Stability; Screech

Generally speaking, afterburning may be considered as a heat addition process in a more or less high-speed gas stream. The one dimensional, steady-flow theory of heat addition in a variable area duct with losses has been given before (Ref. 5 and Ref. 6). The conclusions of this theory may be expressed as follows: Heat can be added in a duct in a steady fashion, or in the more realistic case in a stream tube, until the local Mach number of the flow teaches unity. Then the total head pressure loss and the total temperature reach an extreme value. As it was shown in the above-mentioned reference, the variation of total head pressure loss is as follows:

$$\frac{dP_t}{P_t} = -\frac{\gamma M^2}{2}\left[\frac{dT_t}{T_t} + \frac{2C_f}{\sin 2\theta}\cdot\frac{dA}{A}\right] \qquad (1)$$

Where

P_t = total pressure

T_t = total temperature

γ = specific heat ratio

M = Mach number

A = cross-sectional area

C_f = friction coefficient

θ = slope of the meridian of the duct

This formula suggests that in order to add heat under low pressure losses, the local Mach number of the flow should be kept low. This can only be realized by an increase of the area of the stream tube or the duct area. Such an increase may have an adverse effect on the frontal area of the propulsion system and afterburner cooling.

The main assumptions of the above developed theory were that the flow is steady and the velocity, temperature, etc., distributions were nearly uniform, thus enabling us to treat the problem as one dimensional. Experience shows, however, that neither of these two assumptions is realistic near the sonic velocity because present injector designs do not yield uniform distributions across the duct.

It is well known that at the relatively high temperatures encountered in afterburners, the combustion is unsteady and oscillatory, the combustion taking place always in the turbulent region.

Again because of non-uniform distributions of velocity and temperature, especially near solid obstructions such as flame holders, the Mach number distribution is non-uniform and consequently at certain stream tubes where fuel is available for combustion the Mach number may approach unity.

It is well known (Ref. 7) that no steady transition can occur from a deflagration (subsonic energy release) to a detonation (supersonic energy release); the transition always occurs in an oscillatory fashion. This transonic energy release has been called spinning detonation and has been treated theoretically by Manson (Ref. 8). It has been found that spinning detonation is closely connected with "screech".

Description and physical explanation of the transonic oscillatory phenomenon known as "screech" was given by this author in January 1950. Similar explanations with more mathematical details were given later by Witbeck and by Dennis and Putnam.

"Screech" is a transversal, transonic oscillation which results from non-uniform transversal distribution of velocity and Mach number. This non-uniformity of velocity and temperature is produced and accentuated by the injection and combustion processes. Consequently, the deleterious phenomenon of screech can be avoided or delayed by efficient design of the afterburner in such a way that the injection and combustion processes will produce a uniform velocity and temperature field.

VI Matching and Acceleration

When variable degrees of afterburning are used and the temperature of afterburning and the area of propelling nozzle are known, the "equilibrium lines" of operation may be found if only one such line is known.

As is shown in the Appendix, the "equilibrium running" point on the matching diagram (Figure 5) corresponds to a fictitious non-afterburning turbojet with a fictitious temperature ratio.

$$\left(\sqrt{\frac{T_{5t}}{T_{1t}}}\right)^{*} = \frac{Q_5}{Q_3}\sqrt{\frac{T_{5t}}{T_{1t}}}\sqrt{\frac{T_{5t}}{T_{4t}}}\left(1+\frac{\Delta P_{5t}}{P_{5t}}\right)\left\{\frac{[A_6^{\circ} f(M_6^{\circ})]}{[A_6 f(M_6)]}\right\} \qquad (2)$$

From the above, we may conclude that when the propelling nozzle area A_6 stays constant, afterburning $\left(\sqrt{T_{5t}/T_{4t}} > 1\right)$ results in an increase of the fictitious temperature ratio $\left(T_{5t}/T_{1t}\right)^{*}$ thus raising the equilibrium line of operation, and, if no sufficient margin is available, surging of the compressor may result. This predicament can be remedied however, by an increase of the propelling nozzle area, as is shown in the above formula. From the above, it is obvious that afterburning has the same effect as closing the propelling nozzle. During acceleration the operation point moves toward higher temperature ratio values; consequently, great care should be given during the design of acceleration controls of the injection system to keep the point of operation within the stability limits.

In the case of variable area propelling nozzles this can be effected by linking the acceleration controls with the propelling area controls.

VII Conclusions

The injection process has a great influence upon the operation of afterburning turbojets. With the present lack of fundamental knowledge on injection, empirical design of afterburners is followed by a number of serious limitations, such as altitude flame out, screech, etc.

APPENDIX

Equilibrium running characteristics of afterburning turbojets. The method followed was indicated in Ref. 4. The mass gas flow equation through the propelling nozzle may be given as follows:

$$\frac{Q_5 T_{5t}}{A_6 P_{5t}} = f(M_6) \qquad (1)$$

Where: Q_5 = mass flow rate through the afterburner

T_{5t} = afterburner maximum total gas temperature

P_{5t} = afterburner total pressure

A_6 = propelling nozzle area

$f(M_6)$ = propelling nozzle outlet gas Mach number function

From the above, the following may be obtained:

$$\frac{Q_5}{Q_1} \cdot \frac{Q_1\sqrt{T_{1t}}}{P_{1t}} \cdot \sqrt{\frac{T_{3t}}{T_{1t}}} \cdot \frac{P_{1t}}{P_{3t}} \cdot \frac{P_{3t}}{P_{5t}} = A_6 f(M_6) \qquad (2)$$

Where: Q_1 = air mass flow through the compressor

T_{1t} = total temperature at the compressor inlet

P_{1t}, P_{2t} = total pressure at the compressor inlet and outlet

P_{3t} = total pressure before the turbine

When the total pressure loss in the main combustor and afterburner are ΔP_{23} & ΔP_{45}, the following equations hold true:

$$\frac{P_{3t}}{P_{1t}} = \frac{P_{2t}}{P_{1t}} - \frac{\Delta P_{23}}{P_{1t}} \quad \& \quad \frac{P_{3t}}{P_{5t}} = 1 + \frac{\Delta P_{45}}{P_{5t}} \tag{3}$$

From these, solving for $\frac{P_{3t}}{P_{1t}}$ we obtain:

$$\frac{P_{3t}}{P_{1t}} = \frac{P_{2t}}{P_{1t}} - \frac{\Delta P_{2a}}{P_{1t}} = \frac{Q\sqrt{T_{1t}}}{P_{1t}} \cdot \frac{Q_2}{Q_1} \sqrt{\frac{T_{3t}}{T_{1t}}} \cdot \frac{P_{3t}}{P_{4t}} \cdot \frac{P_{3t}}{P_{5t}} \cdot \frac{1}{A_6 f(M_6)} \tag{4}$$

In the case of turbine choking or near choking the following equation holds true:

$$\frac{P_{4t}}{P_{4t}} = K\sqrt{\frac{T_{3t}}{T_{4t}}} \tag{5}$$

Where:

T_{3t}, T_{4t} = the inlet and outlet turbine total temperature respectively

P_{3t}, P_{4t} = the inlet and outlet turbine total pressure respectively

Consequently, we find:

$$\frac{P_{2t}}{P_{1t}} = \frac{Q_1\sqrt{T_{1t}}}{P_{1t}} \cdot \frac{Q_2}{Q_1} \sqrt{\frac{T_{3t}}{T_{1t}}} \cdot \sqrt{\frac{P_{3t}}{T_{4t}}} \left(1 + \frac{\Delta P_{45}}{P_{5t}}\right) \frac{K}{A_6 f(M_6)} \frac{1}{} + \frac{\Delta P_{2a}}{P_{1t}} \tag{6}$$

In a simple non-afterburning turbojet the following holds true:

$$\frac{P_{2t}}{P_{1t}} = \frac{Q\sqrt{T_{1t}}}{P_{1t}} \cdot \frac{Q_3}{Q_1} \sqrt{\frac{T_{3t}}{T_{1t}}} \cdot \frac{K}{A_6^\circ f(M_6^\circ)} + \frac{\Delta P_{1a}}{P_{1t}} \tag{7}$$

By comparing the above equations it may be seen that the same characteristic equation holds for the afterburning turbojet if a fictitious temperature ratio is considered, as follows:

$$\left(\sqrt{\frac{T_{3t}}{T_{1t}}}\right)^* = \frac{Q_5}{Q_3} \cdot \sqrt{\frac{T_{3t}}{T_{1t}}} \cdot \sqrt{\frac{T_{3t}}{T_{4t}}} \left(1 + \frac{\Delta P_{45}}{P_{5t}}\right) \left\{\frac{A_6^\circ f(M_6^\circ)}{A_6 f(M_6)}\right\} \tag{8}$$

Where the superscript zero indicates non-afterburning and

Q_3 = gas mass flow rate through the turbine

REFERENCES

1. Samaras, D.G. "Thermodynamic Performance Considerations of Jet Propulsion", NRC Report MS-57, February 1942

2. Willcock, R.M. "The Boosting of the Thrust of a Simple Jet Propulsion Turbine Engine", R.A.E. Report #E-4104, February 1944

3. Samaras, D.G. "Comparative Performance of Gas Turbines at Supersonic Forward Speeds", P.J. Report R-1099, June 1945

4. Samaras, D.G. "Present Achievements and Future Developments in Aircraft Gas Turbines", ASME Semi-Annual Meeting, Detroit June 1946

5. Samaras, D.G. "The Problem of Heat Addition in Ducts", Canadian Journal of Research, July 1946

6. Samaras, D.G. "Fluid Dynamics of Energy Release", Fluid Dynamics Panel, University of Illinois, February 1951

7. Samaras, D.G. "Gas Dynamic Treatment of Entothermic and Exothermic Discontinuities", 1948

8. Manson, N. "Propagation des détonations et des déflagrations dans les mélanges gazeux. Paris 1947

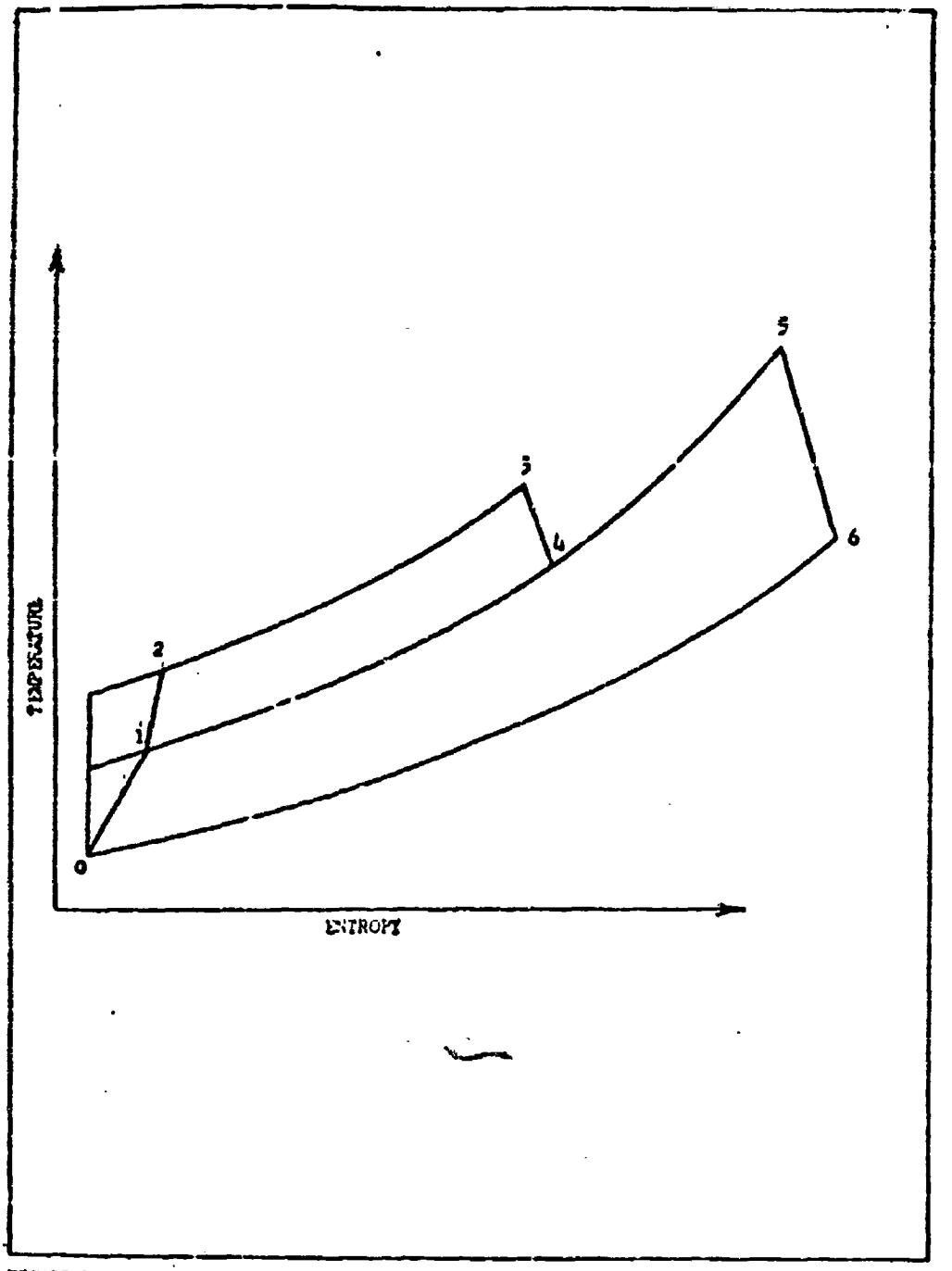

FIGURE 1 – THERMODYNAMIC CYCLE OF AN AFTERBURNING TURBOJET

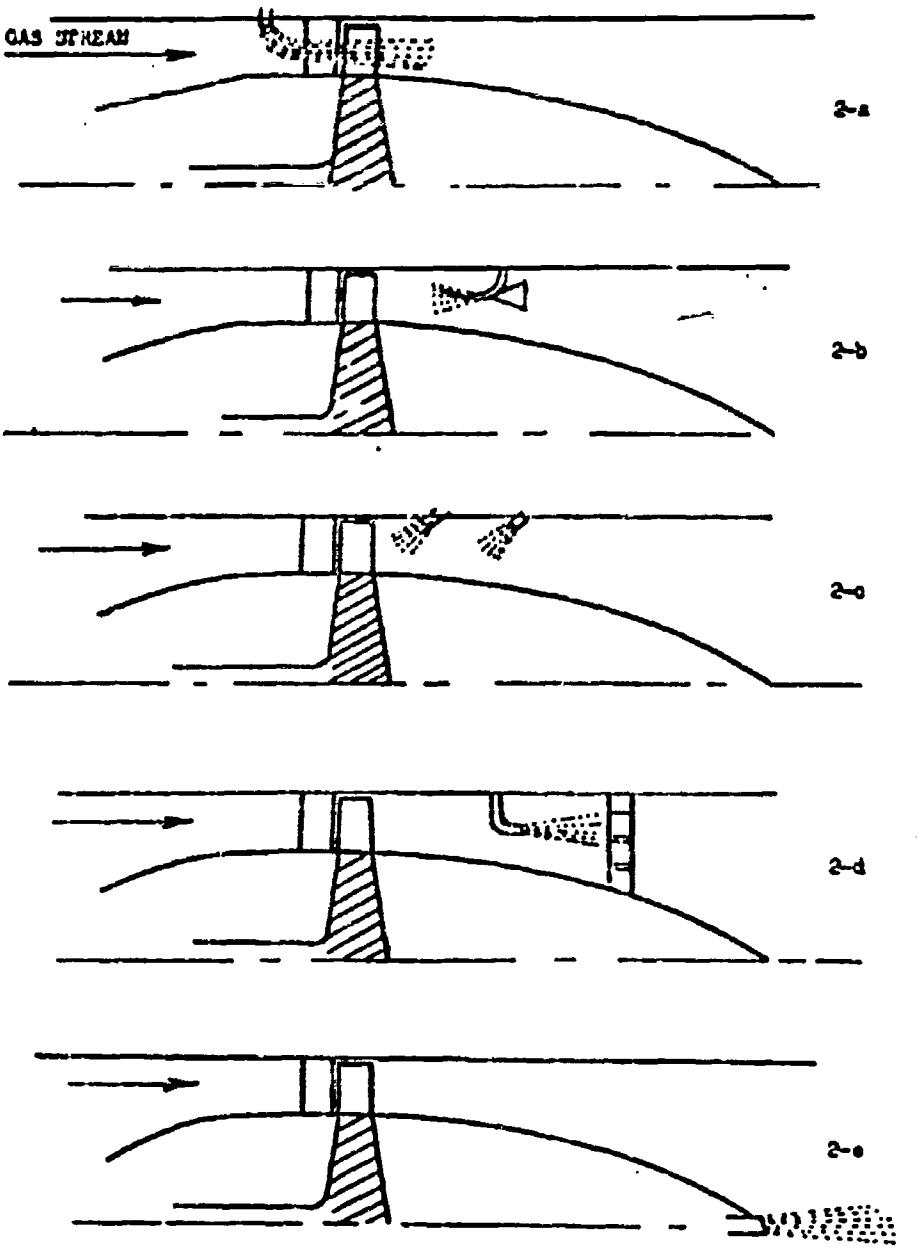

FIGURE 2 – AFTERBURNING TYPES

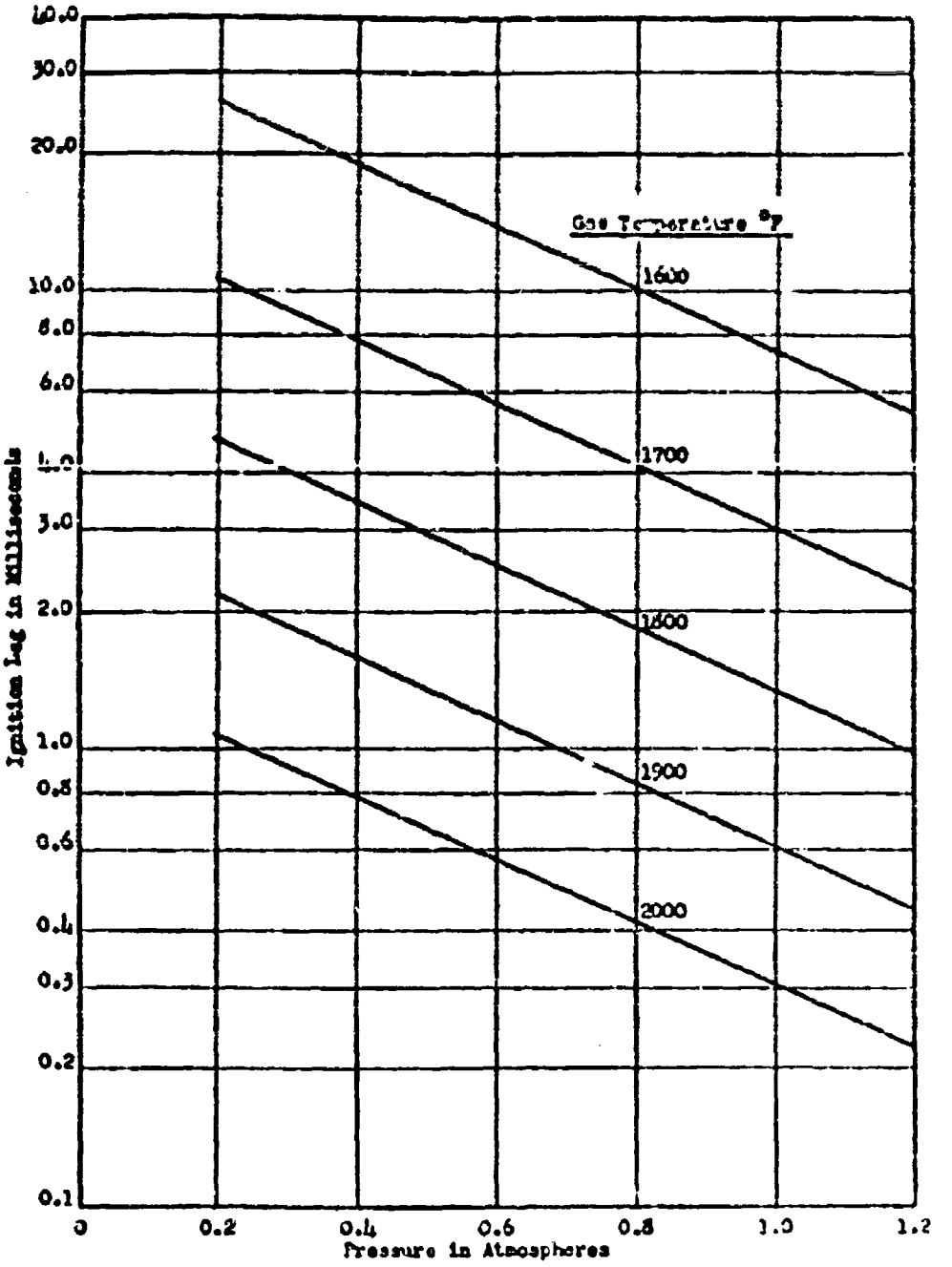

FIGURE 3 VARIATION OF THE IGNITION LAG WITH TEMPERATURE AND PRESSURE

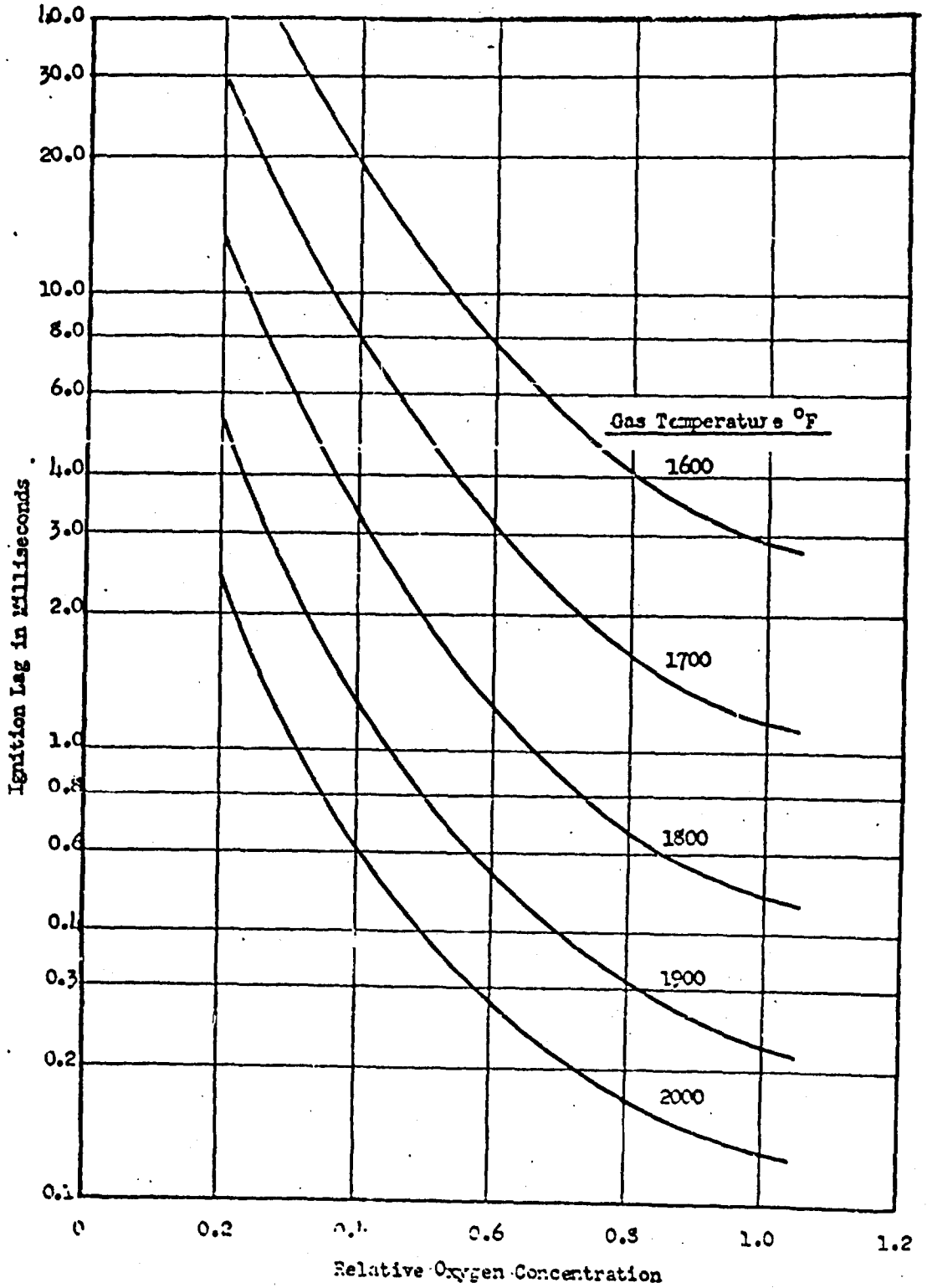

FIGURE 4 VARIATION OF THE IGNITION LAG WITH TEMPERATURE AND OXYGEN DEPLETION.

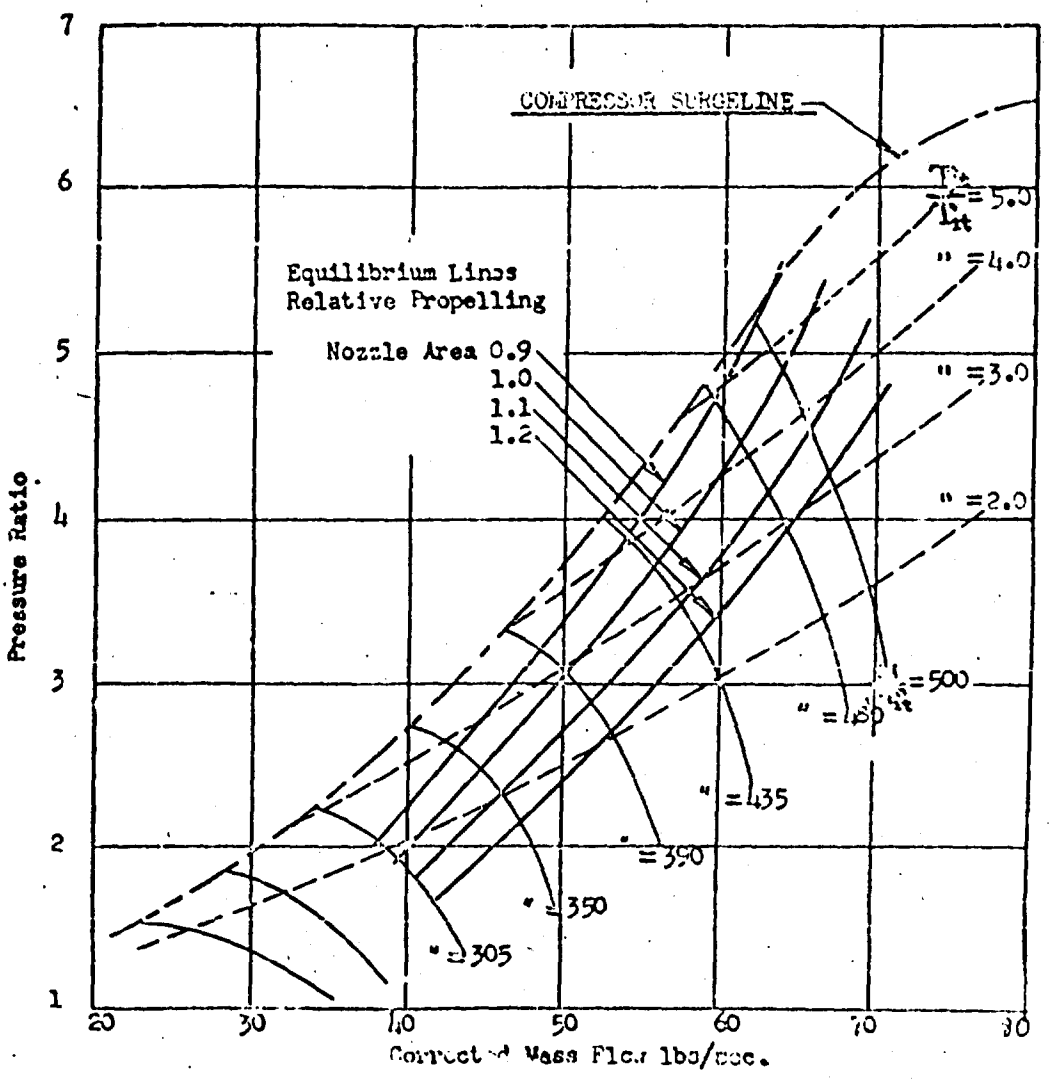

FIGURE 5 – EQUILIBRIUM RUNNING DIAGRAM OF A VARIABLE AREA PROPELLING NOZZLE TURBOJET